

Learning Spectral Windowing Parameters for Regularization Using Unbiased Predictive Risk and Generalized Cross Validation Techniques for Multiple Data Sets

M. J. Byrne and R. A. Renaut

February 7, 2023

MICHAEL J. BYRNE

School of Mathematical and Statistical Sciences
Arizona State University
Tempe, AZ 85287, USA

ROSEMARY A. RENAUT*

School of Mathematical and Statistical Sciences
Arizona State University
Tempe, AZ 85287, USA

Abstract

During the inversion of discrete linear systems noise in data can be amplified and result in meaningless solutions. To combat this effect, characteristics of solutions that are considered desirable are mathematically implemented during inversion, which is a process called regularization. The influence of provided prior information is controlled by non-negative regularization parameter(s). There are a number of methods used to select appropriate regularization parameters, as well as a number of methods used for inversion. New methods of unbiased risk estimation and generalized cross validation are derived for finding spectral windowing regularization parameters. These estimators are extended for finding the regularization parameters when multiple data sets with common system matrices are available. It is demonstrated that spectral windowing regularization parameters can be learned from these new estimators applied for multiple data and with multiple windows. The results demonstrate that these modified methods, which do not require the use of true data for learning regularization parameters, are effective and efficient, and perform comparably to a learning method based on estimating the parameters using true data. The theoretical developments are validated for the case of two dimensional image deblurring. The results verify that the obtained estimates of spectral windowing regularization parameters can be used effectively on validation data sets that are separate from the training data, and do not require known data.

1 Introduction

We consider solutions of ill-conditioned linear problems described by

$$\mathbf{A}\mathbf{x} \approx \mathbf{d}, \quad (1)$$

where $\mathbf{A} \in \mathbb{R}^{m \times n}$ with $m \geq n$ and $\mathbf{d} = \mathbf{b} + \boldsymbol{\eta}$ is measured, with $\boldsymbol{\eta}$ being a realization of a random vector and $\mathbf{b} = \mathbf{A}\mathbf{x}_{\text{true}}$. Even for invertible square matrices direct matrix inversion when \mathbf{A} is ill-conditioned is not recommended due to the noise in the data. Regularization is generally imposed in which desired characteristics of a solution are described mathematically and incorporated into the formulation with the aim to produce a more well-posed problem.

The generalized Tikhonov regularized solution $\mathbf{x}(\alpha)$ [49] is given by

$$\mathbf{x}(\alpha) = \arg \min_{\mathbf{x} \in \mathbb{R}^n} \{ \|\mathbf{A}\mathbf{x} - \mathbf{d}\|_2^2 + \alpha^2 \|\mathbf{L}\mathbf{x}\|_2^2 \}, \quad \alpha > 0, \quad \mathbf{L} \in \mathbb{R}^{q \times n}. \quad (2)$$

The scalar $\alpha > 0$ is a regularization parameter, and \mathbf{L} is a matrix representation of a linear operator. The term $\|\mathbf{L}\mathbf{x}\|_2^2$ is an example of a penalty function [53], and \mathbf{L} is called the penalty matrix. If $\mathbf{L} = \mathbf{I}_n$, the $n \times n$ identity matrix, then regularization via eq. (2) is called standard or zeroth-order Tikhonov regularization [3]. Other standard choices of \mathbf{L} include approximations to first and second order derivative operators [40, 47, 53].

The quality of $\mathbf{x}(\alpha)$ depends on the choice of both α and \mathbf{L} . There are a number of methods for selecting α when \mathbf{L} has been fixed. As an example, the Morozov discrepancy principle (MDP) [38] requires knowledge of the variance of the noise distribution of the data and selects the regularization parameter as the root of a function. The unbiased predictive risk estimator (UPRE) [33] also requires knowledge of the variance of the noise distribution of the data and yields the regularization parameter as the minimizer of a function. The method of generalized cross validation (GCV) [54, 55] does not require the noise distribution be known and also yields the regularization parameter as a minimizer of a function. Some methods do not solve minimization or root-finding problems; for example, the **L – curve** method selects a regularization parameter as the value that locates the point of maximum curvature of a function [23, 26]. As noted, many of these techniques, including the UPRE, MDP, and GCV methods, have statistical foundations [28].

There has been considerable research in selecting sets of regularization parameters for a pre-selected set of penalty matrices, a process called multi-parameter (MP) regularization [7, 12, 18, 32, 57]. Approaches to MP regularization using versions of the **L – curve** and MDP methods can be found in [4] and [56], respectively. An MP GCV method was also considered in [36, 37]. Windowing, either in the data domain or the frequency domain, can also be applied to determine multiple regularization parameters; windowing wavelet coefficients was considered in [16, 46]. Examples of windowed regularization in other frequency domains, such as those generated by discrete trigonometric transforms or the singular value decomposition (SVD), have been presented in [11, 14, 29]. There is also recent work on learning semi-norms as regularization operators [27].

Techniques for utilizing and analyzing multiple data (MD) sets permeate a multitude of scientific fields as diverse as geoscience [6, 58], and cancer detection [45]. A comprehensive overview of data-driven approaches to inverse problems can be found in [2], while specific examples of applying multiple data sets for the solution of inverse problems include [1, 9, 12, 22, 30, 48, 52].

A main contribution of this paper is demonstrating and validating how the functions associated with the **UPRE** and **GCV** methods can be modified to handle multiple data sets, using both scalar and sets of regularization parameters dependent on spectral windows. These are chosen as representative methods that either require (**UPRE**), or do not require (**GCV**), prior knowledge of the statistics of the noise in the data. There is a distinction between the modified methods and those that would use averages of the parameter selection functions; see [8]. Here, the estimators for spectral windowing regularization are derived from first principles. The results show that whereas the **UPRE** method easily extends for spectral windowing regularization, the **GCV** yields an alternative estimator, as was noted already in [11]. The result for the **GCV** was shown for standard form regularization and is here extended for general form Tikhonov regularization. The development of these new methods is presented in Section 3, with proofs of main results in Appendices A and B. Sections 3.1 to 3.2 pertain to the **UPRE** and **GCV** methods, respectively. In addition to developing these modified parameter selection methods, results are presented regarding their relationship(s) with the original method(s) and the simplified expressions for obtaining the required functions using the generalized singular value decomposition are provided for each function. Proofs for the functions and simplified expressions are given in Appendices A to D. The approach using the **UPRE** and **GCV** estimators is contrasted with a machine learning approach relying on the knowledge of true data in Section 4. Numerical results are shown in Section 4. Conclusions are given in Section 5.

Significant Contributions: It is demonstrated through this work how multiple data sets can be used in conjunction with windowed regularization using the formulation introduced in [11]. Windowed parameter versions of the **GCV** method for standard Tikhonov regularization were presented in [11]. Here the windowed **GCV** is derived from first principles for the generalized Tikhonov regularization. The **UPRE** extension is also derived from first principles for standard and generalized Tikhonov regularization. For non-overlapping spectral windows the **UPRE** estimator is separable in the spectral domain, so that windows can be found for each window independently. This is not the case for the **GCV** estimator. Moreover, the windowed **UPRE** follows immediately from the standard formula for the scalar parameter **UPRE** estimate, while the **GCV** function is considerably modified if the leave-one-out approach is strictly applied. Numerical results for the restoration of 2D signalsⁱ, demonstrate that these new windowed regularization parameter estimators can be used for multiple data sets without knowledge of the true data and that their performance competes with a learning approach in which the training stage requires the knowledge of true data. Furthermore, parameters that have been obtained from one set of training images can be used on a separate set of validation (testing) images distinct from the original set, provided that the signal-to-noise ratios are close.

1.1 Summary of notation

Due to the consideration of multiple data sets as well as the windowed parameter regularization for these data sets, the notation in this paper is extensive and will therefore be briefly summarized. We will use the acronym “MD” in the textual body of the paper and plots to refer to the multi-data generalizations, of these methods and their corresponding functions. For example, the MD **UPRE** method means

ⁱResults for 1D problems and all derivations using the **MDP** method are given in [8]

the extension of the UPRE method for multiple data sets, and the notation **win** is used to indicate a function that is defined with respect to regularization parameters used for spectral windows. In the formulation, R denotes the number of data sets being considered, which are indexed by r . The index r may either be placed as a subscript or a superscript with parenthesis signs; for example, $\mathbf{A}^{(r)}$, $\mathbf{x}^{(r)}$, and $\mathbf{d}^{(r)}$ represent the system matrix, solution, and data, respectively, associated with the r th system. The tilde (\sim) is placed above matrices, vectors, or functions to denote their use for MD. Specifically, for matrices the tilde indicates the formation of a block diagonal matrix, e.g. $\tilde{\mathbf{A}} = \text{diag}(\mathbf{A}^{(1)}, \dots, \mathbf{A}^{(R)})$ for $\{\mathbf{A}^{(r)}\}_{r=1}^R$. For vectors, the tilde indicates vertical concatenation, e.g. $\tilde{\mathbf{d}}$ is the ordered vertical concatenation of the vectors $\{\mathbf{d}^{(r)}\}_{r=1}^R$. The functions used in each parameter selection method are indicated using F with subscripts denoting which method is being considered. For example, $\tilde{F}_{\text{UPRE}}(\alpha)$ represents the scalar UPRE function for MD sets. P_r represents the number of windows/parameters being considered for the r th data set; the individual windows are indexed by p , $p = 1 : P$. For matrices, vectors, and functions being used for windowed regularization, the subscript “win” is added. Letters are bolded to indicate vectors; the term $\tilde{F}_{\text{UPRE}}^{\text{win}}(\alpha)$ represents the UPRE function for use in the most general case, where MD are being used for windowed regularization with the parameters contained in the vector α . $\text{null}(\mathbf{A})$ is used to denote the null space of the matrix \mathbf{A} .

2 Regularized Solutions for Single and Multiple Data Sets

We provide first the standard background for determining the solution of the regularized problem eq. (2) for a given scalar regularization parameter α [3, 24]. We then extend this for the solution of eq. (2) using windowing with respect to the spectral domain [11]. Finally, we explain how the scalar and windowed solutions provide a formulation for multiple data sets, as introduced in [12]. For the windowed solutions we assume that the windows in the spectral domain are specified in advance. The aim here is to first show that there is a common framework that can be used to express the solution of the single and multiple data sets problems, for both scalar and windowed formulations. Moreover, we present, as needed, the framework using the generalized singular value decomposition [41], noting that the results simplify for the SVD as is relevant for standard Tikhonov regularization with $\mathbf{L} = \mathbf{I}$ [21].

2.1 The Single Parameter Single Data Set Problem

Under the full column rank assumption for the augmented matrix that defines the normal equations, $\text{null}(\mathbf{A}) \cap \text{null}(\mathbf{L}) = \{\mathbf{0}\}$, the normal equations solution of eq. (2) is given by

$$\mathbf{x}(\alpha) = (\mathbf{A}^\top \mathbf{A} + \alpha^2 \mathbf{L}^\top \mathbf{L})^{-1} \mathbf{A}^\top \mathbf{d} = \mathbf{A}^\#(\alpha) \mathbf{d}, \quad (3)$$

where $\mathbf{A}^\#(\alpha)$ is called the **generalized inverse** matrix [24]. A compact representation for eq. (3) is obtained using the generalized singular value decomposition [41].

Definition 2.1 (The Generalized Singular Value Decomposition (GSVD)). *For real matrices \mathbf{A} and \mathbf{L} of size $m \times n$ and $q \times n$, respectively, and assuming the full column rank condition, the mutual factorizations*

$$\mathbf{A} = \mathbf{U}\mathbf{\Delta}\mathbf{X}^\top, \quad \text{and} \quad \mathbf{L} = \mathbf{V}\mathbf{\Lambda}\mathbf{X}^\top, \quad (4)$$

exist [3]. Here \mathbf{U} is an $m \times m$ orthogonal matrix, \mathbf{V} is a $q \times q$ orthogonal matrix, and \mathbf{X} is an $n \times n$ non-singular matrix. $\mathbf{\Lambda}$ is a $q \times n$ matrix with non-negative diagonal elements in decreasing order on the principal diagonal Λ_{jj} , $1 \leq j \leq \min(q, n) = q^$, and the only elements of the $m \times n$ matrix $\mathbf{\Delta}$ that are possibly non-zero are*

$$0 \leq \Delta_{(1,k+1)} \leq \Delta_{(2,k+2)} \leq \dots \leq \Delta_{(\min(m,n), k+\min(m,n))} \leq 1, \quad k = (n-m)_+.$$

Here $(x)_+$ is defined to be x for $x > 0$ and 0, otherwise.

Equipped with these mutual factorizations, introducing \mathbf{Y} as the inverse of \mathbf{X}^\top , and setting $\hat{\mathbf{d}} = \mathbf{U}^\top \mathbf{d}$, we obtain

$$\mathbf{x}(\alpha) = \mathbf{Y}(\mathbf{\Delta}^\top \mathbf{\Delta} + \alpha^2 \mathbf{\Lambda}^\top \mathbf{\Lambda})^{-1} \mathbf{\Delta}^\top \hat{\mathbf{d}}. \quad (5)$$

But now, with the identity $\mathbf{\Delta}^\top = \mathbf{\Delta}^\top \mathbf{\Delta} \mathbf{\Delta}^\dagger$, where \mathbf{A}^\dagger for a matrix \mathbf{A} is the pseudoinverse of \mathbf{A} [21] and defining $\mathbf{\Phi}(\alpha) = (\mathbf{\Delta}^\top \mathbf{\Delta} + \alpha^2 \mathbf{\Lambda}^\top \mathbf{\Lambda})^{-1} \mathbf{\Delta}^\top \mathbf{\Delta}$, provides the filter matrix representation of eq. (5)

$$\mathbf{x}(\alpha) = \mathbf{Y} \mathbf{\Phi}(\alpha) \mathbf{\Delta}^\dagger \mathbf{U}^\top \mathbf{d}, \quad (6)$$

which also defines $\mathbf{A}^\sharp(\alpha) = \mathbf{Y} \mathbf{\Phi}(\alpha) \mathbf{\Delta}^\dagger \mathbf{U}^\top$.

Examining the entries in the diagonal matrix $\mathbf{\Phi}(\alpha)$, we have

$$\Phi_{jj} = \begin{cases} 0 & j = 1 : \ell \quad (\delta_j = 0) \\ \frac{\delta_j^2}{\delta_j^2 + \alpha^2 \lambda_j^2} & j = \ell + 1 : q^* \\ 1 & j = q^* + 1 : n. \end{cases} \quad (7)$$

Here δ_j and λ_j are defined as follows. Let $\boldsymbol{\delta} = \sqrt{\text{diag}(\mathbf{\Delta}^\top \mathbf{\Delta})}$, (for the element-wise square root), then $\delta_j = \Delta_{(k+1, k+j)}$, $j = 1 : q^*$, and we have defined $\delta_j = 0$, $j = 1 : \ell < n$. Likewise, let $\boldsymbol{\lambda} = \sqrt{\text{diag}(\mathbf{\Lambda}^\top \mathbf{\Lambda})}$, $\lambda_j = \Lambda_{jj}$, $j = 1 : q^*$. Then $\gamma_j = \delta_j / \lambda_j$, $j = 1 : q^*$ are the generalized singular values. Notice $\gamma_j = 0$ for $\delta_j = 0$, and due to the opposite ordering of the δ_j and λ_j , the γ_j are increasing, which is contrary to the standard ordering of the singular values when using the SVD of \mathbf{A} . In the following discussion we assume throughout that $m \geq n$, and that \mathbf{L} has full rank q^* . Therefore $\delta_j = \Delta_{jj}$ and $\Phi_{jj} = \frac{\gamma_j^2}{\gamma_j^2 + \alpha^2}$, $j = 1 : n$ is increasing, with potentially $\Phi_{jj} = 0$ if $\delta_j = \gamma_j = 0$ for $j = 1 : \ell < n$, corresponding also to $(\mathbf{\Phi}(\alpha) \mathbf{\Delta}^\dagger \mathbf{U}^\top \mathbf{d})_j = 0$. Note that according to eq. (7) $\Phi_{jj} = 1$, $j > q^*$.

2.2 Spectral Windowing for the Single Data Set Problem

A more general approach to regularization replaces the scalar regularization parameter by a vector $\boldsymbol{\alpha} = [\alpha_1, \dots, \alpha_P]^\top$ in which α_p is the regularization parameter

for a p^{th} solution obtained with respect to a p^{th} spectral window. These windows are defined, following the approach in [11], using non-negative weights which satisfy

$$\sum_{p=1}^P \mathbf{w}_j^{(p)} = 1, \quad j = 1 : n. \quad (8)$$

We use the index set for a given window $\mathbf{win}^{(p)}$ which is the set of j such that $\mathbf{w}_j^{(p)} \neq 0$. The selection of the windows is predefined and is described in Section 4.1. The diagonal matrices $\mathbf{W}^{(p)} = \text{diag}(\mathbf{w}^{(p)})$, satisfying $\sum_{p=1}^P \mathbf{W}^{(p)} = \mathbf{I}_n$, introduced into eq. (6) yield the windowed solution which is the sum over all P windows

$$\mathbf{x}_{\mathbf{win}}(\boldsymbol{\alpha}) = \sum_{p=1}^P \mathbf{Y}(\mathbf{W}^{(p)})^{1/2} \boldsymbol{\Phi}(\alpha_p) (\mathbf{W}^{(p)})^{1/2} \boldsymbol{\Delta}^\dagger \mathbf{U}^\top \mathbf{d} = \mathbf{Y} \boldsymbol{\Phi}_{\mathbf{win}}(\boldsymbol{\alpha}) \boldsymbol{\Delta}^\dagger \mathbf{U}^\top \mathbf{d}. \quad (9)$$

This defines the symmetric windowed filter matrix and **windowed generalized inverse**

$$\boldsymbol{\Phi}_{\mathbf{win}}(\boldsymbol{\alpha}) = \sum_{p=1}^P (\mathbf{W}^{(p)})^{1/2} \boldsymbol{\Phi}(\alpha_p) (\mathbf{W}^{(p)})^{1/2} = \sum_{p=1}^P \boldsymbol{\Phi}_{\mathbf{win}^{(p)}}(\alpha_p) \quad (10)$$

$$\mathbf{A}_{\mathbf{win}}^\sharp(\boldsymbol{\alpha}) = \mathbf{Y} \boldsymbol{\Phi}_{\mathbf{win}}(\boldsymbol{\alpha}) \boldsymbol{\Delta}^\dagger \mathbf{U}^\top. \quad (11)$$

Furthermore, we may also write the solution as a sum over solutions for each window

$$\mathbf{x}_{\mathbf{win}}(\boldsymbol{\alpha}) = \sum_{p=1}^P \mathbf{Y} \boldsymbol{\Phi}_{\mathbf{win}^{(p)}}(\alpha_p) \boldsymbol{\Delta}^\dagger \mathbf{U}^\top \mathbf{d} = \sum_{p=1}^P \mathbf{A}_{\mathbf{win}^{(p)}}^\sharp(\alpha_p) \mathbf{d} = \sum_{p=1}^P \mathbf{x}^{(p)}(\alpha_p). \quad (12)$$

Defining

$$\mathbf{x}^{(p)}(\alpha_p) = \mathbf{Y} \boldsymbol{\Phi}(\alpha_p) \boldsymbol{\Delta}^\dagger \mathbf{W}^{(p)} \hat{\mathbf{d}}, \quad (13)$$

we notice that $\mathbf{x}^{(p)}(\alpha_p)$ depends only on \hat{d}_j for j in $\mathbf{win}^{(p)}$ when the windows are non-overlapping $\mathbf{w}_j^{(p)} = 1$ for $j \in \mathbf{win}^{(p)}$ and zero otherwise.

2.3 Multiple data sets

Suppose now that we have a collection of data sets $\{\mathbf{d}^{(r)}\}_{r=1}^R$ where, for each data set

$$\mathbf{d}^{(r)} \approx \mathbf{A}^{(r)} \mathbf{x}^{(r)}, \quad (14)$$

analogously to eq. (1), $\mathbf{A}^{(r)} \in \mathbb{R}^{m_r \times n_r}$ with $m_r \geq n_r$, $\mathbf{d}^{(r)} = \mathbf{b}^{(r)} + \boldsymbol{\eta}^{(r)}$, with $\boldsymbol{\eta}^{(r)}$ being a realization of a random vector and $\mathbf{b}^{(r)} = \mathbf{A}^{(r)} \mathbf{x}_{\text{true}}^{(r)}$. For given regularization parameters $\alpha^{(r)}$ and penalty matrices $\mathbf{L}^{(r)}$ of dimension $q_r \times n_r$, Tikhonov regularization can be performed to produce regularized solutions $\mathbf{x}(\alpha^{(r)})$ that minimize the Tikhonov functionals, $\|\mathbf{A}^{(r)} \mathbf{x} - \mathbf{d}^{(r)}\|_2^2 + (\alpha^{(r)})^2 \|\mathbf{L}^{(r)} \mathbf{x}\|_2^2$, which is equivalent to solving eq. (2) but for each system independently.

2.3.1 Scalar Parameter for Multiple Data Sets

Suppose each of the systems are *similar* under some assumptions to be defined as needed, then it may be reasonable to replace $\alpha^{(r)}$ by a common scalar α and seek to find a suitable α for all data sets which can then be used to find solutions for other data sets with *similar* properties. In this framework we consider the determination of

$$\tilde{\mathbf{x}}(\alpha) = \arg \min_{\mathbf{x} \in \mathbb{R}^N} \left\{ \|\tilde{\mathbf{A}}\tilde{\mathbf{x}} - \tilde{\mathbf{d}}\|_2^2 + \alpha^2 \|\tilde{\mathbf{L}}\tilde{\mathbf{x}}\|_2^2 \right\}, \quad (15)$$

for given scalar α , and where we define $N = \sum_{r=1}^R n_r$. Here, with the notation introduced in Section 1.1, $\tilde{\mathbf{x}}$ and $\tilde{\mathbf{d}}$ are the vectors formed by vertically concatenating $\{\tilde{\mathbf{x}}\}_{r=1}^R$ and $\{\mathbf{d}^{(r)}\}_{r=1}^R$, respectively, and matrices $\tilde{\mathbf{A}}$ and $\tilde{\mathbf{L}}$ are the block diagonal matrices generated from $\mathbf{A}^{(r)}$ and $\mathbf{L}^{(r)}$. The advantage of regularizing via eq. (15) is that we only have to select one parameter, α , instead of R parameters (one for each data set). The disadvantage is that we now have to solve a far larger system of equations, and therefore it will be necessary to identify what it means to be *similar*.

First, we observe that we can immediately write down the solution of eq. (15) using the framework in Section 2.1, yielding the solution equivalent to eq. (3) for the large system of equations

$$\tilde{\mathbf{x}}(\alpha) = (\tilde{\mathbf{A}}^\top \tilde{\mathbf{A}} + \alpha^2 \tilde{\mathbf{L}}^\top \tilde{\mathbf{L}})^{-1} \tilde{\mathbf{A}}^\top \tilde{\mathbf{d}} = \tilde{\mathbf{A}}^\#(\alpha) \tilde{\mathbf{d}}. \quad (16)$$

This is a completely separable block diagonal solution, common only through α . As for the single data set case, it is convenient to introduce the assumption that there is a GSVD for each system, as given in Assumption 1.

Assumption 1 (GSVD for matrix pair $\mathbf{A}^{(r)}, \mathbf{L}^{(r)}$). *We assume that there exist matrices $\mathbf{\Delta}^{(r)} \in \mathbb{R}^{m_r \times n_r}$ and $\mathbf{\Lambda}^{(r)} \in \mathbb{R}^{q_r \times n_r}$ such that $\mathbf{A}^{(r)} = \mathbf{U}^{(r)} \mathbf{\Delta}^{(r)} (\mathbf{X}^{(r)})^\top$ and $\mathbf{L}^{(r)} = \mathbf{V}^{(r)} \mathbf{\Lambda}^{(r)} (\mathbf{X}^{(r)})^\top$ for $r = 1 : R$, where $\mathbf{U}^{(r)}$ and $\mathbf{V}^{(r)}$ are orthogonal, $\mathbf{X}^{(r)}$ is invertible and $\text{null}(\mathbf{A}^{(r)}) \cap \text{null}(\mathbf{L}^{(r)}) = \{\mathbf{0}\}$.*

So far this imposes no *similarity* between systems but allows the solution to be written in the filtered form, equivalent to eq. (6),

$$\tilde{\mathbf{x}}(\alpha) = \tilde{\mathbf{Y}} \tilde{\mathbf{\Phi}}(\alpha) \tilde{\mathbf{\Delta}}^\dagger \tilde{\mathbf{U}}^\top \tilde{\mathbf{d}} = \tilde{\mathbf{A}}^\#(\alpha) \tilde{\mathbf{d}}, \quad (17)$$

Note this also defines $\tilde{\mathbf{A}}^\#(\alpha) = \tilde{\mathbf{Y}} \tilde{\mathbf{\Phi}}(\alpha) \tilde{\mathbf{\Delta}}^\dagger \tilde{\mathbf{U}}^\top$. Again the notation from Section 1.1 is applied. This extends the result in [12, Eq. 3.14] to the case when $\mathbf{\Delta}$ need not be invertible. Strictly speaking we do not need to use the GSVD for these solutions, but it is the use of the spectral information provided by the GSVD, or SVD when the operator \mathbf{L} is replaced by the identity, that facilitates in the context of our analysis the definition of a windowed solution dependent on the generalized singular values, respectively singular values if $\mathbf{L} = \mathbf{I}$. We observe that $\tilde{\mathbf{\Phi}}$ is symmetric block diagonal with diagonal blocks. We reiterate that eqs. (16) and (17) are no more than eqs. (3) and (6), respectively, simply applied for the large system of equations with no assumptions about any common system information.

2.3.2 Windowing for Multiple Data Sets

Having provided the spectral windowing for the single data set, it is now immediate that we could apply windowing to each of the r data sets. Let $\alpha^{(r)} =$

$[\alpha_1^{(r)}, \alpha_2^{(r)}, \dots, \alpha_{P_r}^{(r)}]$ be the P_r regularization parameters used for windowed regularization applied to the r th system described by eq. (14). Then, as in eq. (9), the independently constructed regularized solutions yield the filter representation for each solution

$$\mathbf{x}_{\text{win}}^{(r)}(\boldsymbol{\alpha}^{(r)}) = \mathbf{Y}^{(r)} \boldsymbol{\Phi}_{\text{win}}^{(r)}(\boldsymbol{\alpha}^{(r)}) (\boldsymbol{\Delta}^{(r)})^\dagger (\mathbf{U}^{(r)})^\top \mathbf{d}^{(r)}.$$

Here $\boldsymbol{\Phi}_{\text{win}}^{(r)}$ incorporates the independent window weighting matrices as in eq. (10) and is again symmetric. As in eq. (11) we could define the appropriate generalized inverse matrices for each system. If each system has its own set of windows, there are a total of $\sum_{r=1}^R P_r$ regularization parameters. Instead we introduce additional assumptions.

Assumption 2 (Windows and $\boldsymbol{\alpha}$). *We assume*

1. the number of windows P_r is the same for each system, i.e $P_r = P$ for all $r = 1 : R$ and $\boldsymbol{\alpha}^{(r)} \in \mathbb{R}^P$, $r = 1 : R$.
2. $\boldsymbol{\alpha}^{(r)} = \boldsymbol{\alpha}$, $r = 1 : R$.

By the first statement of Assumption 2 there are RP parameters. Now as for the scalar case, the solution of the problems defined for these concatenated systems is equivalent to solving each independently. But the second statement of Assumption 2 reduces the number of unknowns to P and introduces taking advantage of multiple systems to find an optimal vector $\boldsymbol{\alpha}$. Note, this still does not imply that the windows need to be the same. In summary we have the standard filtered form for the concatenated solution, as in eq. (9),

$$\tilde{\mathbf{x}}_{\text{win}}(\boldsymbol{\alpha}) = \tilde{\mathbf{Y}} \tilde{\boldsymbol{\Phi}}_{\text{win}}(\boldsymbol{\alpha}) \tilde{\boldsymbol{\Delta}}^\dagger \tilde{\mathbf{U}}^\top \tilde{\mathbf{d}} = \tilde{\mathbf{A}}_{\text{win}}^\dagger \tilde{\mathbf{d}}, \quad (18)$$

in which the diagonal weighting matrices are hidden within $\tilde{\boldsymbol{\Phi}}_{\text{win}}$, and $\tilde{\mathbf{A}}_{\text{win}}^\dagger$ is defined as in eq. (11).

3 Parameter selection methods

An estimate of scalar α can be found by applying many different criteria for defining what it means for α to be *optimal*, and there are numerous descriptions in the literature [3, 24, 53]. Here, to find α we focus on the method of generalized cross validation (GCV), [54, 55] and the unbiased predictive risk estimator (UPRE), [33, 53]. While both techniques are statistically based, the GCV does not rely on any knowledge of the statistical distribution for $\boldsymbol{\eta}$, but for the UPRE we need to assume $\boldsymbol{\Sigma}^{(r)}$, the covariance matrix for the noise in sample r , is available. For eq. (2) these methods require the minimization of an objective function that depends on the scalar α . We present the standard UPRE and GCV functions to find α for $R = 1$ and then derive the extensions of the UPRE and GCV functions for the determination of the *optimal* $\boldsymbol{\alpha}$ for the windowed MD solution eq. (18). The proofs of the main results are provided in Appendices A and B, and the derivations which use the GSVD to simplify the terms that are used to calculate the underlying functions to be minimized dependent on $\boldsymbol{\alpha}$ are given in Appendix C.

3.1 The Unbiased Predictive Risk Estimator

The UPRE method was developed in 1973 by Mallows and considers the statistical relationship between the regularized residual $\mathbf{r}(\alpha) = \mathbf{A}\mathbf{x}(\alpha) - \mathbf{d}$, and the predictive error $\mathbf{p}(\alpha) = \mathbf{A}(\mathbf{x}(\alpha) - \mathbf{x}_{\text{true}})$. Assuming $\Sigma = \sigma^2 \mathbf{I}_m$, the standard UPRE objective function for Tikhonov regularization is given by

$$F_{\text{UPRE}}(\alpha) = \frac{1}{m} \|\mathbf{r}(\alpha)\|_2^2 + \frac{2\sigma^2}{m} \text{trace}(\mathbf{A}(\alpha)) - \sigma^2 \quad (19)$$

[53, p. 98] and the optimal α is defined by

$$\alpha_{\text{UPRE}} = \arg \min_{\alpha > 0} F_{\text{UPRE}}(\alpha). \quad (20)$$

In eq. (19) $\mathbf{A}(\alpha)$ is the data resolution matrix

$$\mathbf{A}(\alpha) = \mathbf{A}(\mathbf{A}^\top \mathbf{A} + \alpha^2 \mathbf{L}^\top \mathbf{L})^{-1} \mathbf{A}^\top = \mathbf{A} \mathbf{A}^\#(\alpha), \quad (21)$$

and $F_{\text{UPRE}}(\alpha)$ is an unbiased estimator of the expected value of the predictive risk, $\frac{1}{m} \|\mathbf{p}(\alpha)\|_2^2$. The derivation of the UPRE function for the most general case with P windows and R data sets follows the details for the derivation of eq. (19) as given in [53, p. 98], under the additional assumption on the data sets that $\boldsymbol{\eta}^{(r)}$, $r = 1 : R$, are mutually independent. We collect the required assumptions in Assumption 3.

Assumption 3 (The Data Sets). *For $r = 1 : R$, assume that $\mathbf{b}^{(r)} = \mathbf{A}^{(r)} \mathbf{x}^{(r)}$, $\mathbf{d}^{(r)} = \mathbf{b}^{(r)} + \boldsymbol{\eta}^{(r)}$, and $\boldsymbol{\eta}^{(r)} \sim \mathcal{N}(\mathbf{0}^{(r)}, \Sigma^{(r)})$ with mutually independent $\boldsymbol{\eta}^{(r)}$. Equivalently, $\boldsymbol{\eta}^{(r)}$ follows a Gaussian distribution with mean $\mathbf{0}$ and symmetric positive definite covariance matrix $\Sigma^{(r)}$. The vectors $\mathbf{b}^{(r)}$, $\mathbf{d}^{(r)}$, and $\boldsymbol{\eta}^{(r)}$ are of length m_r and $\mathbf{x}^{(r)}$ is of length n_r .*

Theorem 3.1 (UPRE function for multiple data sets and multiple windows). *Under Assumptions 2 and 3, and assuming that each $\mathbf{A}_{\text{win}}^{(r)}(\alpha) = \mathbf{A}^{(r)}(\mathbf{A}_{\text{win}}^{(r)})^\#$, $r = 1 : R$, is symmetric, then the UPRE function $\tilde{F}_{\text{win}}^{\text{UPRE}}(\alpha)$ for the data sets $\{\mathbf{d}^{(r)}\}_{r=1}^R$ with windows $\{\{\mathbf{W}^{(r,p)}\}_{p=1}^P\}_{r=1}^R$ is*

$$\tilde{F}_{\text{win}}^{\text{UPRE}}(\alpha) = \frac{1}{M} \sum_{r=1}^R m_r F_{\text{win}}^{(r)}(\alpha), \quad (22)$$

where

$$F_{\text{win}}^{(r)}(\alpha) = \frac{1}{m_r} \|\mathbf{r}_{\text{win}}^{(r)}(\alpha)\|_2^2 + \frac{2}{m_r} \text{trace}(\Sigma^{(r)} \mathbf{A}_{\text{win}}^{(r)}(\alpha)) - \frac{1}{m_r} \text{trace}(\Sigma^{(r)}), \quad (23)$$

and $M = \sum_{r=1}^R m_r$.

Proof. The proof is given in Appendix A. \square

In Theorem 3.1 there is no assumption made that the windows used are the same, nor that the systems are of the same size, namely, we do not assume $m_r = m$, $r = 1 : R$. Moreover, the results are given in terms of the generalized inverse matrix trace terms and the residuals for each system, without any use of the GSVD for the matrix pairs $\mathbf{A}^{(r)}$ and $\mathbf{L}^{(r)}$.

It is immediate that eq. (22) does not align with eq. (19), in particular, each of the functions for system r are more general than eq. (19). To relate the two expressions we assume either $\mathbf{\Sigma}^{(r)} = \sigma_r^2 \mathbf{I}_{m_r}$, where σ_r^2 is the common variance in the noise, or that the Gaussian noise is whitened by applying the whitening, or zero-phase component analysis (ZCA) [5], transformation $(\mathbf{\Sigma}^{(r)})^{-1/2}$ to eq. (14) for each r .

Assumption 4 (Mutually Independent Whitened Data). *We assume $\mathbf{\Sigma}^{(r)} = \sigma_r^2 \mathbf{I}_{m_r}$, $r = 1 : R$. If the ZCA transform is applied to whiten the r^{th} data set we have $\sigma_r^2 = 1$*

Corollary 3.1.1 (UPRE for mutually independent data). *Under Assumption 4*

$$F_{\text{win}}^{\text{UPRE}}(\boldsymbol{\alpha}) = \frac{1}{m_r} \|\mathbf{r}_{\text{win}}^{(r)}(\boldsymbol{\alpha})\|_2^2 + \frac{2}{m_r} \sigma_r^2 \text{trace}(\mathbf{A}_{\text{win}}^{(r)} \boldsymbol{\alpha}) - \sigma_r^2. \quad (24)$$

Proof. This is immediate by using $\mathbf{\Sigma}^{(r)} = \sigma_r^2 \mathbf{I}_{m_r}$ in eq. (23). \square

Finally, if we have systems that are all of the same size, $m_r = m$, the fraction m_r/M simplifies as $1/R$ and we obtain

$$\tilde{F}_{\text{win}}^{\text{UPRE}}(\boldsymbol{\alpha}) = \frac{1}{R} \sum_{r=1}^R F_{\text{win}}^{\text{UPRE}}(\boldsymbol{\alpha}). \quad (25)$$

Remark 1 (Comment on symmetry for the data resolution matrices). *It is clear from the proof given in Appendix A that it is not necessary to assume symmetry in order to evaluate the estimator, this is only needed to combine the two terms. To be more general we obtained the first steps of the proof without the symmetry requirement. Yet, we can also obtain symmetry without using a mutual spectral decomposition for \mathbf{A} and \mathbf{L} . Indeed, returning to the normal equations form eq. (3) for the solution, without windowing, we can introduce the diagonal matrices $\mathbf{W}^{(p)}$ directly to define a p^{th} solution dependent on $\mathbf{W}^{(p)}$ and a scalar regularization parameter α_p ,*

$$\mathbf{x}^{(p)}(\alpha_p) = (\mathbf{W}^{(p)})^{1/2} (\mathbf{A}^\top \mathbf{A} + \alpha_p^2 \mathbf{L}^\top \mathbf{L})^{-1} (\mathbf{W}^{(p)})^{1/2} \mathbf{A}^\top \mathbf{d} = \mathbf{A}_p^\#(\alpha_p) \mathbf{d}. \quad (26)$$

The data resolution matrix associated with eq. (26) is immediately symmetric, and it reduces to the original windowed form for $\mathbf{x}^{(p)}(\alpha_p)$ when the GSVD is applied. Still, the more general expression eq. (26) facilitates an alternative direction for finding multiple regularization parameters based on blocks of components in $\mathbf{A}^\top \mathbf{d}$, such as using domain multisplitting [42, 44]. The expression is also relevant when it is not feasible to find a mutual spectral decomposition but it is possible to implement forward operations with matrices \mathbf{A} and \mathbf{L} . Noting that the proof of Theorem 3.1 does not make any assumptions about the use of the GSVD, we reiterate that Theorem 3.1 provides a UPRE form that can be used more generally.

We now focus on the use of mutual spectral decompositions for \mathbf{A} and \mathbf{L} that can be used to simplify the expressions used to estimate $\boldsymbol{\alpha}$ as the solution of eq. (20) applied for eq. (22). The standard approach uses the GSVD (or the SVD when $\mathbf{L} = \mathbf{I}$) that is also relevant for Kronecker product forms for \mathbf{A} and \mathbf{L} . Discrete Fourier or cosine transforms (DCT) also provide a mutual decomposition that can

be employed. Here we give the results in terms of the GSVD, and will show how it can be used in Section 4. The proofs of elementary algebraic results are given in Appendix C. The relation of the DCT to the GSVD is given in Appendix D

For the single data set case with windowing, and introducing the diagonal matrix $\mathbf{\Psi} = \mathbf{I} - \mathbf{\Phi}$, Lemmas C.2 to C.3 immediately provide

$$\|\mathbf{r}_{\text{win}}(\boldsymbol{\alpha})\|_2^2 = \sum_{j=1}^{q^*} \left(\sum_{p=1}^P w_j^{(p)} \Psi_{jj}(\alpha_p) \right)^2 \hat{d}_j^2 + \sum_{j=n+1}^m \hat{d}_j^2, \quad (27)$$

and

$$\text{trace}(\mathbf{A}_{\text{win}}(\boldsymbol{\alpha})) = (n - q^*) + \sum_{j=\ell+1}^{q^*} \sum_{p=1}^P w_j^{(p)} \Phi_{jj}(\alpha_p), \quad (28)$$

respectively. Hence, ignoring constant terms, and using the index (r, p) to indicate data set r and window p , we can write

$$\begin{aligned} \tilde{F}_{\text{win}}^{\text{UPRE}}(\boldsymbol{\alpha}) = \frac{1}{M} \sum_{r=1}^R \left(\sum_{j=1}^{q_r^*} \left(\sum_{p=1}^P w_j^{(r,p)} \Psi_{jj}^{(r)}(\alpha_p) \right)^2 \left(\hat{d}_j^{(r)} \right)^2 + \right. \\ \left. 2\sigma_r^2 \sum_{j=\ell+1}^{q_r^*} \sum_{p=1}^P w_j^{(r,p)} \Phi_{jj}^{(r)}(\alpha_p) \right). \end{aligned} \quad (29)$$

Likewise, for non-overlapping windows using Lemmas C.2 and C.3, ignoring constant terms we obtain a function for each window,

$$\tilde{F}_{\text{win}}^{\text{UPRE}(p)}(\alpha_p) = \frac{1}{M} \left(\sum_{r=1}^R \sum_{j \in \text{win}^{(r,p)}} \left(\Psi_{jj}^{(r)}(\alpha_p) \hat{d}_j^{(r)} \right)^2 + 2\sigma_r^2 \sum_{j \in \text{win}^{(r,p)}} \Phi_{jj}^{(r)}(\alpha_p) \right). \quad (30)$$

Finally, combining eqs. (29) and (30) we have the main result to estimate the windowed regularization parameters using R measurements $\mathbf{d}^{(r)}$ for unknown $\mathbf{x}^{(r)}$, $r = 1 : R$ given the GSVD for the system \mathbf{A} with penalty matrix \mathbf{L} . In this case $m_r = m$, $n_r = n$, $q_r^* = q^*$, $M = Rm$, and we assume that the same windows are used for each system.

Proposition 3.1. *Under Assumptions (2) to (4), with now $\mathbf{A}^{(r)} = \mathbf{A}$, $\mathbf{L}^{(r)} = \mathbf{L}$ and $\boldsymbol{\Sigma} = \boldsymbol{\Sigma}^{(r)} = \sigma^2 \mathbf{I}_m$, the windowed parameter vector $\boldsymbol{\alpha}$ for the UPRE function, after removing the common factor $1/m$ is*

$$\begin{aligned} \boldsymbol{\alpha}_{\text{UPRE}} = \arg \min_{\boldsymbol{\alpha} \in \mathbb{R}_+^P} \left\{ \frac{1}{R} \sum_{r=1}^R \left(\sum_{j=1}^{q^*} \left(\sum_{p=1}^P w_j^{(p)} \Psi_{jj}(\alpha_p) \right)^2 \left(\hat{d}_j^{(r)} \right)^2 + \right. \right. \\ \left. \left. 2\sigma^2 \sum_{j=\ell+1}^{q^*} \sum_{p=1}^P w_j^{(p)} \Phi_{jj}(\alpha_p) \right) \right\}. \end{aligned} \quad (31)$$

For non-overlapping windows α can be found by minimizing for each scalar parameter α_p independently using the frequency domain data $\hat{\mathbf{d}}^{(r)}$, $r = 1 : R$

$$\alpha_p = \arg \min_{\alpha > 0} \left\{ \frac{1}{R} \sum_{r=1}^R \left(\sum_{j \in \text{win}(p)} \left(\Psi_{jj}(\alpha) \hat{d}_j^{(r)} \right)^2 \right) + 2\sigma^2 \sum_{j \in \text{win}(p)} \Phi_{jj}(\alpha) \right\}. \quad (32)$$

3.2 Generalized Cross Validation

In contrast to the UPRE function, the GCV function does not require knowledge of the covariance matrix Σ . Yet, it is statistically based, and is obtained by applying a leave-one-out analysis. It yields the function

$$F_{\text{GCV}}(\alpha) = \frac{\frac{1}{m} \|\mathbf{r}(\alpha)\|_2^2}{\left(\frac{1}{m} \text{trace}(\mathbf{I}_m - \mathbf{A}(\alpha)) \right)^2} = \frac{\frac{1}{m} \|\mathbf{r}(\alpha)\|_2^2}{\left(1 - \frac{1}{m} \text{trace}(\mathbf{A}(\alpha)) \right)^2}, \quad (33)$$

for which we define

$$\alpha_{\text{GCV}} = \arg \min_{\alpha > 0} F_{\text{GCV}}(\alpha). \quad (34)$$

It is immediate that we can define α_{GCV} for the concatenated systems, assuming a leave-one-out-analysis applied for the system defined by $\tilde{\mathbf{A}}$, replacing m by M and the residual and trace terms calculated for $\tilde{\mathbf{A}}$. On the other hand, it was shown in [11] that the immediate application of eq. (33) for the system described by the single system with windowing is not consistent with the leave-one-out analysis. Rather, deriving the GCV for the windowed system from first principles, assuming the standard Tikhonov regularization with $\mathbf{L} = \mathbf{I}_n$, yields a new function [11, Theorem 3.2] which is more complex algebraically. Applying the same analysis from first principles based on the Allen Press function, [19], for the generalized Tikhonov form, we arrive at the following result which expands on [11, Theorem 3.2].

Theorem 3.2 (Windowed GCV Function for a single data set). *Assume \mathbf{L} has full rank (row rank if $q < n$ but column rank if $q \geq n$), $\lambda_j > 0$, $j = 1 : q^*$, $m \geq n$, and $0 = \delta_1 = \dots = \delta_\ell < \delta_{\ell+1} \dots \leq \delta_n$. The windowed GCV function for the generalized Tikhonov regularization is given by*

$$F_{\text{GCV}}^{\text{win}}(\alpha) = \frac{1}{m} \left(\sum_{j=q^*+1}^m \left(1 + \left(\sum_{p=1}^P \frac{1 - \nu_p}{\mu_p} \right) \right)^2 \hat{d}_j^2 + \sum_{j=1}^{q^*} \left(1 + \left(\sum_{p=1}^P \frac{1 - \nu_p}{\mu_p} \right) - \left(\sum_{p=1}^P \frac{1}{\mu_p} \frac{\gamma_j^2 w_j^{(p)}}{\gamma_j^2 + \alpha_p^2} \right) \right)^2 \hat{d}_j^2 \right). \quad (35)$$

Here the number of windows is P , the weights on each window for generalized singular value γ_j are given by $w_j^{(p)}$, and μ_p and ν_p are obtained from Lemma B.1 as

$$\mu_p = \frac{1}{m} \left(m - n + q^* - \sum_{j=1}^{q^*} \frac{\gamma_j^2}{\gamma_j^2 + \alpha_p^2} \right) \quad \text{and} \quad \nu_p = \frac{1}{m} \left(m - n + q^* - \sum_{j=1}^{q^*} \frac{\gamma_j^2 w_j^{(p)}}{\gamma_j^2 + \alpha_p^2} \right).$$

Note that $\Phi_{jj} = 1$ for $j > q^*$ and so some terms in the summation cancel when $q^* < n$. The same applies for $(\Phi_{\text{win}(p)}(\alpha_p))_{jj}$, also with $w_j^{(p)} = 0$.

In contrast to the analysis for the **UPRE**, the derivation and associated proof, as given in Appendix B, for Theorem 3.2 relies explicitly on the availability of a mutual spectral decomposition for \mathbf{A} and \mathbf{L} . In [11] the equivalent result relied on the use of the SVD and made the assumption that all singular values are positive. The result here explicitly permits $\delta_j = 0 = \gamma_j$, and is sufficiently general that it applies for the case when \mathbf{L} is tall or wide. On the other hand, as noted in [11], eq. (35) is a complicated non-linear function of P variables, and it can be beneficial to consider alternative approximations for finding a good **GCV** type estimator for α . There, it is suggested that non-overlapping windows can be used to find a good initial point for optimization, in which case a **GCV** function for each window can be optimized separately for scalar α_p . Here we consider this approach, but also compare with an estimator that is obtained by applying the standard **GCV** function in which the residual and trace terms in the numerator and denominator are calculated directly. Having provided Theorem 3.2 it is immediate, as already noted, that this estimator is not a true **GCV** estimator for the windowed case.

First we note that in the scalar parameter case, eq. (33) generalizes to

$$\tilde{F}_{\text{GCV}}(\alpha) = \frac{\frac{1}{M} \|\tilde{\mathbf{r}}(\alpha)\|_2^2}{\left(1 - \frac{1}{M} \text{trace}(\tilde{\mathbf{A}}(\alpha))\right)^2} \quad (36)$$

for the MD case with $M = \sum_{r=1}^R m_r$. When using non-overlapping windows, from eq. (36) and $\tilde{\mathbf{A}}_{\text{win}}(\alpha) = \tilde{\mathbf{A}} \tilde{\mathbf{A}}_{\text{win}}^\#$ we can select α_p for $p = 1 : P$ using the independent functions

$$\tilde{F}_{\text{EstGCV}_{\text{win}}}^{(p)}(\alpha_p) = \frac{\frac{1}{M} \|\hat{\tilde{\mathbf{r}}}_{\text{win}}^{(p)}(\alpha_p)\|_2^2}{\left(1 - \frac{1}{M} \text{trace}(\tilde{\mathbf{A}} \tilde{\mathbf{A}}_p^\#)\right)^2}, \quad (37)$$

with $\hat{\tilde{\mathbf{r}}}_{\text{win}}^{(p)}(\alpha_p) = \tilde{\mathbf{U}}^\top \tilde{\mathbf{A}} \tilde{\mathbf{x}}^{(p)}(\alpha_p) - \tilde{\mathbf{W}}^{(p)} \tilde{\mathbf{U}}^\top \tilde{\mathbf{d}}$. Equation (37) can also be applied to a single data set $\mathbf{d} \in \mathbb{R}^m$ and non-overlapping windows (the tilde notation is dropped and M replaced by m). The use of eq. (37) is analogous to [10, eq. 3.13] extended to the MD environment; eq. (37) is not a true **GCV** function, though minimization is easier than minimizing eq. (35). As with the derivations of the **UPRE** functions in section 3.1, eq. (37) can also be written in terms of the GSVD using the results in Appendix C. Finally, we note, as with the **UPRE**, that having estimators for the scalar and windowed parameter solutions immediately provides the estimators for the block systems of equations for multiple data sets.

4 Numerical Experiments

To evaluate the effectiveness of the spectral windowing and scalar parameter selection methods described in Section 3, we present the results for a single two dimensional test problem, with different noise levels and blur width. Results for one dimensional problems are presented in [8]. For both problems the parameter(s) are found for a set of training data, and then validated using a separate validation set. The results for the 1D problem, which serves as a proof of concept for the methods and that use MRI data that is built into MATLAB[®], are detailed in [8].

More relevant are the results for the two-dimensional problem which is described in detail here. This problem utilizes the images in fig. 1 of the planet Mercury obtained by the MESSENGER space probeⁱⁱ. The signal-to-noise ratio (SNR) is

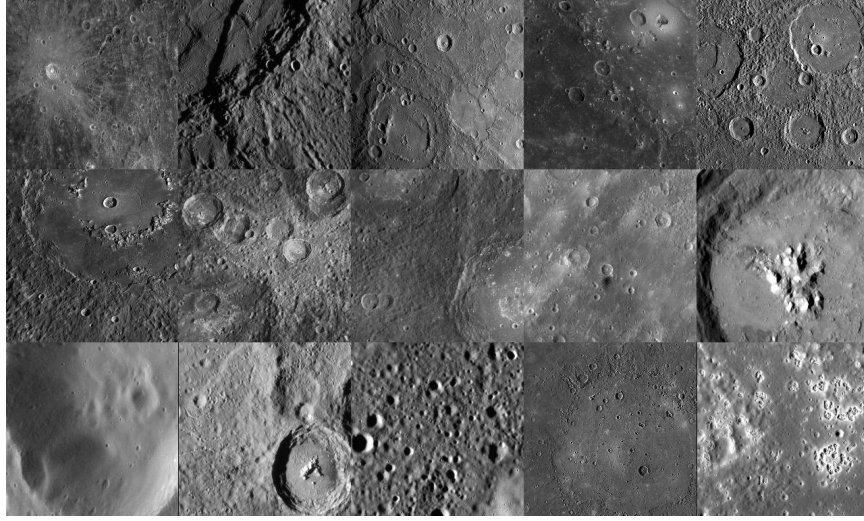


Figure 1: Selected images used for MESSENGER 2D test problem. Available courtesy of NASA/JPL-Caltech [39].

used as a measurement for noise content in the images and is given by

$$\text{SNR} = 10 \log_{10} \left(\frac{\mathcal{P}_{\text{signal}}}{\mathcal{P}_{\text{noise}}} \right).$$

In the discrete setting, the average power \mathcal{P} of a vector \mathbf{x} of length n is defined as $\frac{1}{n} \|\mathbf{x}\|_2^2$. Using this definition for vectors \mathbf{b} and $\boldsymbol{\eta}$, $\mathcal{P}_{\text{signal}} = \frac{1}{m} \|\mathbf{b}\|_2^2$ and $\mathcal{P}_{\text{noise}} = \frac{1}{m} \|\boldsymbol{\eta}\|_2^2$ and so the quotient in the logarithm is $\|\mathbf{b}\|_2^2 / \|\boldsymbol{\eta}\|_2^2$. If \mathbf{b} is a matrix representing an image, in which case $\boldsymbol{\eta}$ is a realization of a random matrix, the 2-norm can be replaced by the Frobenius norm.

For a basis of comparison, parameters were also selected as minimizers of the *learning* function

$$\tilde{F}_{\text{win}}^{\text{MSE}}(\boldsymbol{\alpha}) = \frac{1}{R} \|\tilde{\mathbf{x}}_{\text{win}}(\boldsymbol{\alpha}) - \tilde{\mathbf{x}}\|_2^2 = \frac{1}{R} \sum_{r=1}^R F_{\text{win}}^{\text{MSE}}(r)(\boldsymbol{\alpha}), \quad (38)$$

where

$$F_{\text{win}}^{\text{MSE}}(r)(\boldsymbol{\alpha}) = \|\mathbf{x}_{\text{win}}^{(r)}(\boldsymbol{\alpha}) - \mathbf{x}^{(r)}\|_2^2. \quad (39)$$

Note that this definition requires that the true solutions, $\{\mathbf{x}^{(r)}\}_{r=1}^R$, are known, as it finds the parameters to minimize the mean squared relative error (MSE) using

ⁱⁱThe selected MESSENGER images are available to the public courtesy of NASA and JPL-Caltech [39]. The identifiers of the images in fig. 1, starting from the top row and moving left to right, are: PIA10173, PIA10174, PIA10177, PIA10942, PIA11246, PIA12042, PIA12068, PIA12116, PIA14189, PIA15756, PIA18372, PIA19024, PIA19203, PIA19213, PIA19267.

known data. Regularization parameters chosen as minimizers of eq. (38) are *optimal* in the sense of minimizing the MSE of the regularized solutions $\mathbf{x}_{\text{win}}^{(r)}(\boldsymbol{\alpha})$; the use of eq. (38) was considered in [12]. One could also find minimizers $\boldsymbol{\alpha}^{(r)}$ of eq. (39) for each $r = 1 : R$, which would produce parameters that are *optimal* for their own data set. In the results we use MSE to indicate results that are found using the learning function eq. (39).

In the experiments we use the spectral windows as described in Section 4.1 and to evaluate the forward operators we use the Kronecker product 2D discrete cosine transform (DCT). The relation of the 1D DCT to the GSVD is briefly described in Section 4.2. The extension that relates the Kronecker product 2D DCT to the KP GSVD follows similarly.

4.1 Spectral Windows

In the experiments we use windowing following the approach in [11]. First we consider non-overlapping windows, $\mathbf{W}^{(p)}$, for which the components of their corresponding weight vectors $\mathbf{w}^{(p)}$ satisfy

$$\mathbf{w}_j^{(p)} \in \{0, 1\}, \quad j = 1 : n, \quad p = 1 : P. \quad (40)$$

The condition given by eq. (40) means that for each $j = 1 : n$, there is exactly one $p \in \{1 : P\}$ such that $\mathbf{w}_j^{(p)} = 1$.

Perhaps the simplest way of choosing the components of $\mathbf{w}^{(p)}$ is to first choose $P + 1$ partition values $\omega^{(0)} \geq \dots \geq \omega^{(P)}$ such that $\omega^{(0)} \geq s_1$ and $s_n > \omega^{(P)}$, then for $p = 1 : P$, the non-zero components occur for those j for which s_j is in the p^{th} window:

$$\mathbf{w}_j^{(p)} = 1, \text{ for } \omega^{(p-1)} \geq s_j > \omega^{(p)}. \quad (41)$$

Here s_j correspond to the generalized singular values, ordered in the opposite order, decreasing rather than increasing. This is consistent with the standard ordering of the singular values when using the SVD of the matrix \mathbf{A} . The partition values $\omega^{(0)} \geq \dots \geq \omega^{(P)}$ used in the experiments are formed by taking $P + 1$ linearly or logarithmically equispaced samples of the interval $[\gamma_1, \gamma_n^*]$, where γ_n^* is a largest non-infinite generalized singular value of (\mathbf{A}, \mathbf{L}) . Partition values can also be used to generate overlapping windows. For example, cosine windows are defined in [11, Eq. 3.6-3.7] by using midpoints of each partition. Linearly and logarithmically spaced cosine windows are used in the experiments as examples of overlapping windows.

4.2 The DCT

While the GSVD is useful for analyzing problems with a general matrix \mathbf{A} , for practical image deblurring problems with $m_r = n_r$ it is more computationally efficient to use the 2D discrete cosine transform (DCT). Assuming that reflexive boundary conditions are applied, primarily to reduce the potential for reflection that would arise with zero boundary conditions, then both \mathbf{A} and \mathbf{L} have the same block structure and the DCT can be used to simultaneously diagonalize \mathbf{A} and \mathbf{L} into a BTTB + BTHB + BHTB + BHBB matrix, with the ‘‘T’’ and ‘‘H’’ standing for Toeplitz and Hankel, respectively, [25]. Theorem 4.1, for which a brief proof is given in Appendix D, describes how a simultaneous diagonalization of these matrices is related to their GSVD.

Theorem 4.1. *GSVD for the DCT [8] Given the simultaneous diagonalization of the $n \times n$ symmetric matrices $\mathbf{A} = \mathbf{C}^\top \tilde{\mathbf{\Delta}} \mathbf{C}$ and $\mathbf{L} = \mathbf{C}^\top \tilde{\mathbf{\Lambda}} \mathbf{C}$ where \mathbf{C} is orthogonal and $\text{null}(\mathbf{A}) \cap \text{null}(\mathbf{L}) = \{\mathbf{0}\}$, \mathbf{A} and \mathbf{L} can be expressed as $\mathbf{A} = \mathbf{U} \mathbf{\Delta} \mathbf{X}^\top$ and $\mathbf{L} = \mathbf{U} \mathbf{\Lambda} \mathbf{X}^\top$, respectively, where \mathbf{U} is orthogonal, \mathbf{X} is invertible, $\mathbf{\Delta}^\top \mathbf{\Delta} + \mathbf{\Lambda}^\top \mathbf{\Lambda} = \mathbf{I}_n$, $0 \leq \Delta_{1,1} \leq \dots \leq \Delta_{n,n} \leq 1$, and $1 \geq \Lambda_{1,1} \geq \dots \geq \Lambda_{n,n} \geq 0$.*

Theorem 4.1 serves as a theoretical tool that bridges different matrix decompositions for the purpose of forming a greater variety of implementation options. Specifically, this result assists in the efficient implementation for the regularization estimators, both **UPRE** and **GCV**, using the simplified expressions for the results in Appendices A to C. While Theorem 4.1 applies to any simultaneous diagonalization of symmetric matrices, the **DCT** has the advantage of avoiding complex operations that would generally arise if using fast Fourier transforms, rather than the **DCT**. Naturally, we could also impose zero boundary conditions or periodic boundary conditions [25]. Our choice to use the **DCT** is not generally limiting but appropriate for the given application.

4.3 Two-dimensional problems

The data sets for the 2D test problem consist of images of size 256×256 . A total of 16 images were used and split into training and validation sets containing 8 images each. To obtain the 16 images from the 512×512 Mercury images in fig. 1, the first 8 images were chosen and two 256×256 subimages of each image were selected as the northwest and southeast corners. Another validation set of images, shown in fig. 2, was used that consisted of built-in MATLAB[®] images.

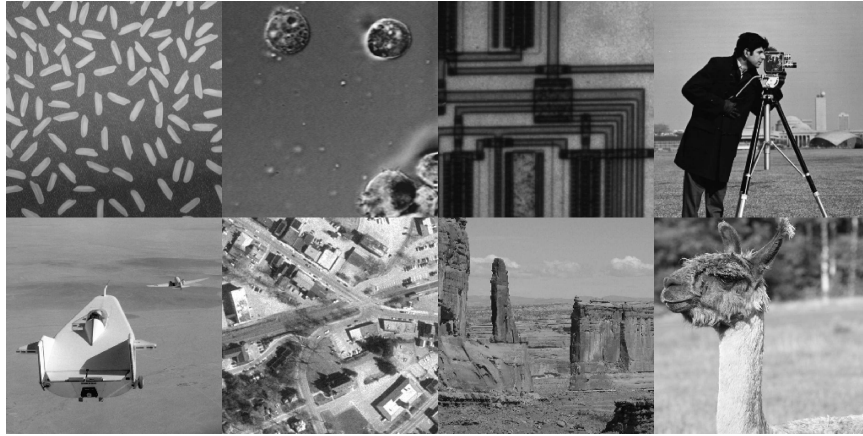


Figure 2: The second validation set, consisting of built-in MATLAB[®] images. From left to right starting in the top row, the images are: `rice.png`, `AT3_1m4_01.tif`, `circuit.tif`, `cameraman.tif`, `liftingbody.png`, `westconcordorthophoto.png`, `parkavenue.jpg`, and `llama.jpg`.

A 256×256 point spread function was formed using a discretization of the zero centered, circularly symmetric Gaussian kernel, $k(x, y) = \exp(-(x^2 + y^2)/(2\xi))$. The parameter ξ controls the width of the Gaussian kernel. Choosing $k(x, y)$ to

be circularly symmetric is for convenience; a Gaussian kernel with different width parameters for the x and y directions can still be used to construct $k(x, y)$ that is doubly symmetric for diagonalization via the DCT [25]. In regards to the value of ξ , values $\xi = 4, 16$, and 36 correspond to blurring that is referred to as “mild,” “medium,” and “severe”, respectively, [17]. The corresponding $k(x, y)$ were discretely convolved with each image as a means of blurring. SNR values of 10, 25 and 40 were used to construct mean zero independent Gaussian noise vectors that were added to the blurred images to create the data. For one choice of the penalty matrix \mathbf{L} , we used the appropriately structured version of the discrete negative Laplacian operator, which is an approximation of the continuous Laplacian operator [15, 31], and which we denote by $\mathbf{L} = \mathbf{L}_2$. For the second penalty matrix we used $\mathbf{L} = \mathbf{I}$. The structure of \mathbf{A} and \mathbf{L} allows for simultaneous diagonalization using the DCT for numerical efficiency (see Section 4.2).

The learning methods were evaluated for both the scalar and spectral windowing cases using training data sets of sizes $R = 1$ to 8. The learned parameters in each case were then used to construct regularized solutions for data from two independent validation sets. For the windowed regularization we considered both non-overlapping linear/logarithmic windows and overlapping linear/logarithmic cosine windows. The decision to use linear spacing for $\mathbf{L} = \mathbf{I}$ and logarithmic spacing for $\mathbf{L} = \mathbf{L}_2$ is supported by how the ordered spectral components decay [8]. As in [11], the windowed GCV function eq. (35) was replaced by the P independent approximate GCV functions eq. (37) for simplicity when considering non-overlapping windows. Parameters were also obtained for the separable UPRE method given by eq. (30). For the spectral windowing with overlapping windows, the minimizations were initialized using the parameters obtained by the non-overlapping methods. Overall, in terms of the choice to initialize the parameters for the overlapping windows with parameters obtained from the separable case, we note that the windowed UPRE and GCV methods corresponding to overlapping windows performed better when the minimizations were initialized using the parameter obtained by the non-overlapping methods. Results without this initialization are not given.

Considering first the scalar parameter MD case, the resulting parameters appear to stabilize as the number of data sets is increased. Figure 3 demonstrates this effect and shows that the amount of stabilization appears to be connected to the homogeneity of the training set. Sets constructed from fig. 1 are homogeneous in the sense that they all contain images of the surface of Mercury. In contrast, fig. 2 consisted of entirely distinct images. By changing which sets are used for training or validation influences the resulting parameters as R increases. The corresponding relative errors of the regularized solutions are shown in fig. 4. While the box plots in fig. 4(a) and fig. 4(b) simply look as if they are the same but reordered, the box plots appear similar because the resulting parameters are approximately the same ($\alpha \approx 0.2$). These experiments suggest that it is sufficient to use only a small number of images, relative to the total available, to obtain meaningful results. The use of fig. 2 as a training set was only considered to produce fig. 3 and fig. 4; its use as a validation set is retained through the remainder of the results.

In regards to the spectral windowing, typically two windows were sufficient (corresponding to the use of just two parameters in the windowed estimators) to obtain meaningful solutions. The observed benefit of using greater than two windows was minor, an example of which is shown for the windowed UPRE method in fig. 5(a). Another advantage of using two windows is that there is a greater computational

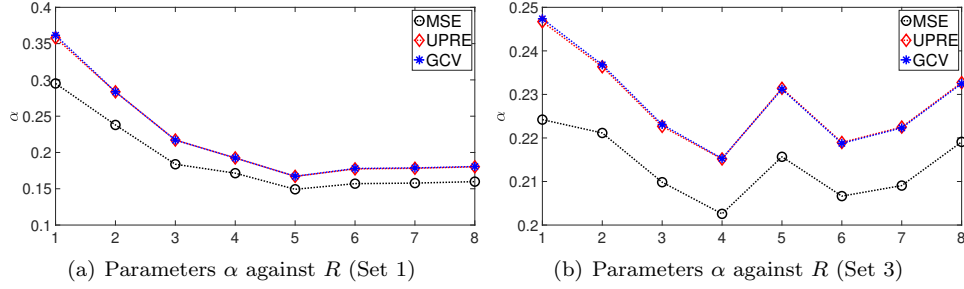


Figure 3: Figure 3(a) illustrates the change in scalar α as the number of data sets increases, here with Set 1 as the training set and in fig. 3(b) with Set 3 (see fig. 4). Figure 3(a) is an example of how scalar regularization parameters can stabilize as the number of data sets in the MD methods increases. In contrast, fig. 3(b) shows less stabilization with increasing R when the training set is changed. For both plots, $\xi = 16$, $\mathbf{L} = \mathbf{L}_2$, and an SNR of 25 was used.

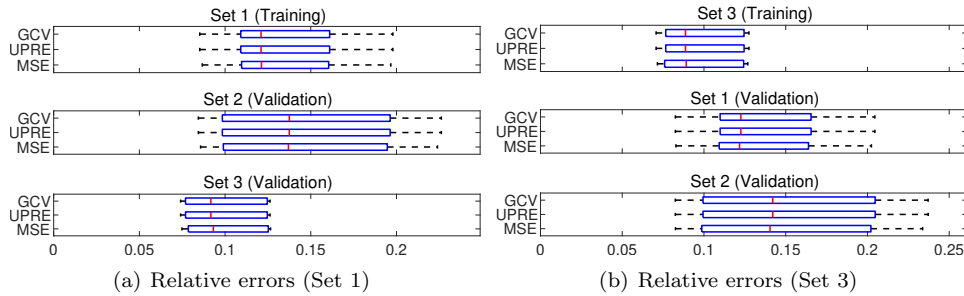


Figure 4: Relative errors of regularized solutions obtained for scalar α from each MD method with $R = 5$ data sets. Here Set 1 and Set 2 were constructed from fig. 1, while Set 3 was constructed from fig. 2. In fig. 4(a), Set 1 served as the training set and the resulting parameters were used to construct solutions for the data from Sets 2 and 3. Figure 4(b) shows results where training was done using Set 3 instead and Sets 1 and 2 served as validation sets. For both plots, $\xi = 16$, $\mathbf{L} = \mathbf{L}_2$, and an SNR of 25 was used.

cost of finding more parameters than is necessary for meaningful regularized solutions; this is especially true for overlapping windows where decoupling is not an option. Extending the number of windows also has the effect of reducing the influence of one or more parameters. For example, fig. 5(b) shows that one of the three parameters obtained from the windowed UPRE method with three windows is more variable and larger in magnitude than that other two parameters.

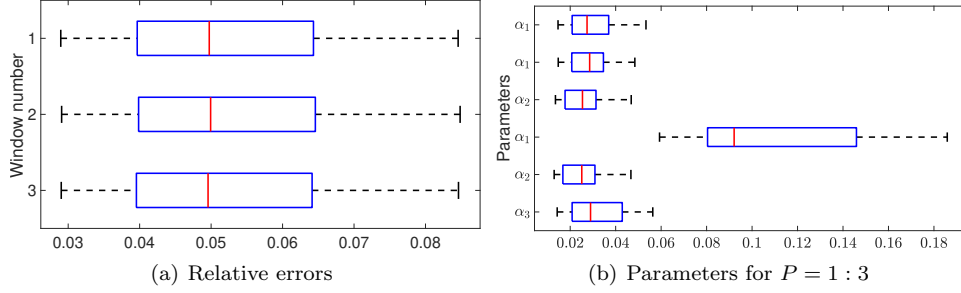


Figure 5: Parameters and corresponding relative errors from the UPRE method as the number of windows is increased from one to three. Figure 5(a) shows that there is little benefit in using an increasing number of windows. Figure 5(b) shows that past two windows, the new regularization parameters are more variable. For both plots, logarithmically spaced windows were used with $\xi = 4$, $\mathbf{L} = \mathbf{L}_2$, and an SNR of 40.

The results presented in [11] also suggested that there is little to be gained when using more than two windows, even when using the learning approach, method MSE, to find the parameters. On the other hand, the presented framework is valid for more windows, should there be situations in which the use of two windows seems insufficient based on numerical experiments. It should be noted also, that when using the MD windowed MDP method, there is an additional tuning safety parameter, which is required and makes the presentation of results for the MDP method much less interesting, see [8].

The use of overlapping or non-overlapping windows influences the degree of interdependence between the two parameters. Figure 6 presents the results of using overlapping and non-overlapping logarithmic windows with $\mathbf{L} = \mathbf{L}_2$. When using non-overlapping windows, the ranges of both parameters are smaller than those for non-overlapping windows. For overlapping windows, the behavior of α_1 exhibited in fig. 6 shows the parameters grouping near 10. The grouping behavior can be explained by the choice of an upper bound during the minimization process; in the case of fig. 6, the upper bound was chosen near 10. The calculated gradients of the $F_{\text{win}}^{\text{MSE}}(\alpha)$, $F_{\text{win}}^{\text{UPRE}}(\alpha)$, and $F_{\text{win}}^{\text{GCV}}(\alpha)$ are too small to resolve a minimum in the direction of α_2 and thus the minimization process determines the minimizers near the specified boundary. However, using overlapping windows also increased the magnitude of α_2 , most significantly in the case of the GCV method.

In regards to the MD windowed methods, which select P parameters using R data sets, the parameters converge as R increases. Table 1 details the mean percent relative errors of solutions obtain using parameters from each MD windowed method, where one and two (both overlapping and non-overlapping) windows were used. Even for the limited number of training sets (2 through 8), the errors decrease

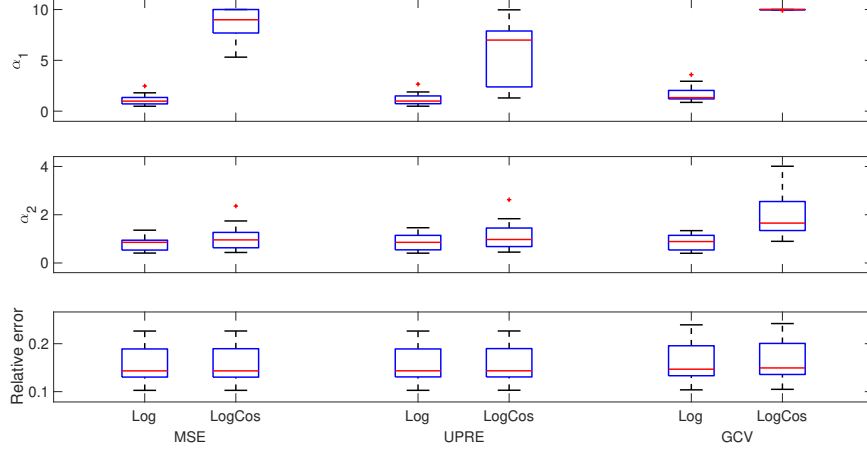


Figure 6: Parameters and corresponding relative errors obtained from using logarithmic vs logarithmic-cosine windows with the **MSE**, **UPRE**, and **GCV** methods. In the case of the logarithmic (non-overlapping) windows, the independent versions of the **UPRE** and **GCV** functions were used, eqs. (30) and (37), respectively. For both window versions, $\xi = 4$, $\mathbf{L} = \mathbf{L}_2$, and an SNR of 10 was used.

as R increases. For most numerical configurations tested, the use of overlapping vs non-overlapping windows provides minor benefit with regards to the relative errors of the regularized solutions.

It is interesting to note that the average relative errors of solutions obtained for parameters applied to the second validation set (fig. 2) were less than those of either the training or first validation set. The superior (reduced) errors calculated for the second validation set are consistent throughout most numerical configurations. Additionally, the relative errors for the second validation set show greater variability than those for either the training, or first validation, set. Furthermore, the relative errors are indeed least in each case when training is performed using known data, namely with the **MSE**, but the results with both **UPRE** and **GCV** learning methods are not significantly larger when using windowed regularization. This demonstrates that windowed regularization parameters can be learned from training data without knowledge of the true solutions. The results obtained using **UPRE** are in most cases slightly improved as compared to those using **GCV**, and hence **UPRE** would be preferred if information about the noise in the data is available. Finally, to illustrate the performance of the approach, fig. 7 presents two examples of images from the second validation set that have differing relative errors.

5 Conclusions

We have shown that the **UPRE** and **GCV** methods can be extended to accommodate regularization parameter estimation using multiple data sets and for both single and windowed regularization parameters, for generalized Tikhonov regularization. The **UPRE** is a representative estimator that assumes the knowledge of the variance of mean zero Gaussian noise in the data, while no additional assumptions are required for the **GCV** estimator. The most general forms of functions associated with these

Table 1: Averaged percent relative errors of the MD windowed regularized solutions for $\xi = 36$ and an SNR of 10 with one window, two linearly spaced windows and two linearly spaced cosine windows with the identity penalty matrix. The result with least error for given R , method, and validation set is highlighted in bold face.

R	Win	Training			Validation 1			Validation 2		
		MSE	UPRE	GCV	MSE	UPRE	GCV	MSE	UPRE	GCV
2	None	21.32	25.83	25.87	23.76	27.58	27.62	17.57	23.27	23.32
	Lin	19.64	19.54	19.54	22.85	22.67	22.67	14.94	14.88	14.89
	LinCos	19.54	19.93	19.94	22.83	23.38	23.39	14.78	15.10	15.11
4	None	21.29	26.09	26.12	23.71	27.82	27.86	17.58	23.57	23.62
	Lin	19.44	19.53	19.55	22.39	22.36	22.37	14.93	15.16	15.17
	LinCos	19.32	19.33	19.94	22.32	22.29	23.39	14.75	14.79	15.11
6	None	21.29	26.03	26.07	23.71	27.77	27.81	17.58	23.51	23.56
	Lin	19.44	19.49	19.50	22.41	22.36	22.37	14.91	15.05	15.07
	LinCos	19.32	19.32	19.94	22.34	22.34	23.39	14.73	14.72	15.11
8	None	21.29	26.02	26.06	23.71	27.76	27.80	17.57	23.50	23.55
	Lin	19.44	19.48	19.49	22.41	22.36	22.37	14.90	15.04	15.06
	LinCos	19.32	19.32	19.94	22.34	22.34	23.39	14.72	14.72	15.11

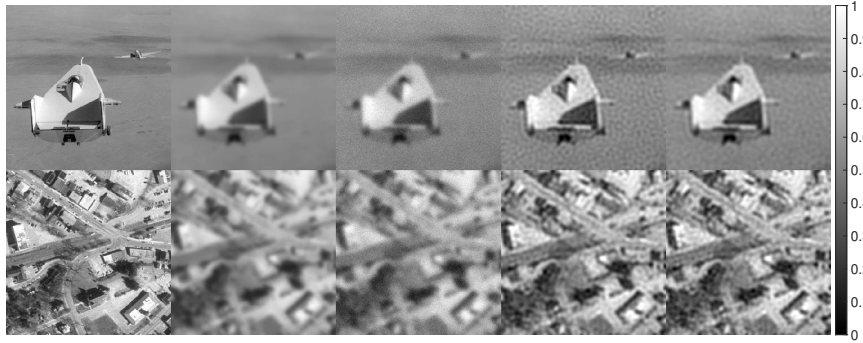


Figure 7: Two samples from the second validation set, with $\xi = 36$, an SNR of 25, two log cosine windows and the Laplacian penalty matrix. From left to right for each sample are the true solution, the blurred image, the blurred image after noise was added, the regularized solution obtained using the MD windowed UPRE method with $R = 8$ (the entire training set), and the regularized solutions using parameters that are optimal for the individual image. The MD windowed UPRE solutions have relative errors of 8.55% and 14.81% for the top and bottom samples, respectively, while the optimal solutions have relative errors of 8.04% and 14.80%.

methods are given in Theorem 3.1 and Theorem 3.2. While the corresponding function for the MD windowed **UPRE** can be written as an average of the individual functions associated with each data set, this is not possible for the MD windowed **GCV**. Moreover, the **GCV** estimator for windowed regularization parameters when derived from first principles is more complex, and unlike the **UPRE** case, does not yield a separable form when non-overlapping windows are applied. Still, neither of these MD windowed methods require knowledge of true solutions unlike the learning approach defined by eq. (38). The presented numerical experiments for 2D signal restoration demonstrate that the MD windowed methods can perform competitively with the learning approach that requires knowledge of true signals for training from data. Further, it is also demonstrated that the parameters obtained from a specific training set of validation images can also be used for a set of different testing images, provided that the general noise characteristics are the same. Varying the noise characteristics of the training and/or validation sets could be an interesting approach for future investigation.

We note that the approach discussed here will extend immediately for any estimator which relies only on an approximation for the regularized residual and the trace of the data resolution matrix, as is the case for **UPRE**, provided that the derivation from first principles still leads to an equivalent formulation for the function that should be minimized. The general idea can be modified to address estimators requiring other terms, such as an augmented regularized residual used for the χ^2 estimator described in [34, 35], and as already given in [8] for the **MDP** method. Although the implementation is presented for the case in which there is a known mutual decomposition of the model and penalty matrices (**A** and **L**) the approach can be extended for any iterative method which yields suitable estimates, e.g. [13, 43, 50, 51]. In particular, the assumption of a mutual diagonalization is only a simplifying assumption that is useful computationally for the **UPRE** method. Consequently, the approach here can also be used with other Kronecker product representations for the model and penalty matrices, or for Krylov methods that can be used to provide a spectral representation of the two operators. Such extensions would be a topic for future research, as would a true multi penalty regularization using multiple data sets for learning parameters to meet conditions for **UPRE**. We conclude that the results are particularly helpful in demonstrating that **UPRE** offers a major advantage, as compared to **GCV**; the derivation from first principles yields a standard **UPRE** function, whereas the **GCV** does not. This suggests that **UPRE** will be of more general use in conjunction with iterative solvers replacing the direct solves, which is not the case for the **GCV** formulation. Moreover, **UPRE** is immediately separable for non-overlapping windows but **GCV** is not.

References

- [1] Babak Maboudi Afkham, Julianne Chung, and Matthias Chung. Learning regularization parameters of inverse problems via deep neural networks. *Inverse Problems*, 37(10):105017, sep 2021.
- [2] S. Arridge, P. Maass, O. Öktem, and Carola-Bibiane Schönlieb. Solving inverse problems using data-driven models. *Acta Numerica*, 28:1–174, 2019.
- [3] R C Aster, B Borchers, and C H Thurber. *Parameter Estimation and Inverse Problems*. Elsevier, Amsterdam, 2nd edition, 2013.

- [4] Murat Belge, Misha E Kilmer, and Eric L Miller. Efficient determination of multiple regularization parameters in a generalized L-curve framework. *Inverse Problems*, 18:1161–1183, July 2002.
- [5] Anthony J. Bell and Terrence J. Sejnowski. The “independent components” of natural scenes are edge filters. *Vision Research*, 37:3327–3338, December 1997.
- [6] Karianne J Bergen, Paul A Johnson, Maarten V de Hoop, and Gregory C Beroza. Machine learning for data-driven discovery in solid earth geoscience. *Science*, 363, March 2019.
- [7] C. Brezinski, M. Redivo-Zaglia, G. Rodriguez, and S. Seatzu. Multi-parameter regularization techniques for ill-conditioned linear systems. *Numerische Mathematik*, 94:203–228, 2003.
- [8] Michael J. Byrne. *Adaptive methods for the selection of regularization parameters*. PhD thesis, Arizona State University, January 2022.
- [9] J Chung, M Chung, and D P O’Leary. Designing optimal spectral filters for inverse problems. *SIAM Journal on Scientific Computing*, 33:3131–3135, 2011.
- [10] Julianne Chung, Glenn Easley, and Dianne O’leary. Windowed spectral regularization of inverse problems. *SIAM J. Scientific Computing*, 33:3175–3200, 01 2011.
- [11] Julianne Chung, Glenn Easley, and Dianne P. O’Leary. Windowed spectral regularization of inverse problems. *SIAM Journal on Scientific Computing*, 33(6):3175–3200, 2011.
- [12] Julianne Chung and Malena I Español. Learning regularization parameters for general-form Tikhonov. *Inverse Problems*, 33(7):074004, 2017.
- [13] Julianne Chung, James G Nagy, and Dianne P O’Leary. A weighted GCV method for Lanczos hybrid regularization. *Electronic Transactions on Numerical Analysis*, 28:149–167, 2008.
- [14] Julianne M. Chung, Misha E. Kilmer, and Dianne P. O’Leary. A framework for regularization via operator approximation. *SIAM Journal on Scientific Computing*, 37(2):B332–B359, 2015.
- [15] Lokenath Debnath and Piotr Mikusiński. *Introduction to Hilbert Spaces with Applications*. Elsevier, 3rd edition, September 2005.
- [16] Glenn R. Easley, Demetrio Labate, and Vishal M. Patel. Directional multi-scale processing of images using wavelets with composite dilations. *Journal of Mathematical Imaging and Vision*, 48:13–34, January 2014.
- [17] Silvia Gazzola, Per Christian Hansen, and James G. Nagy. IR Tools: A MATLAB package for iterative regularization methods and large-scale problems. *Numerical Algorithms*, 81:773–811, July 2019.
- [18] Silvia Gazzola and Paolo Novati. Multi-parameter Arnoldi-Tikhonov methods. *Electronic Transactions on Numerical Analysis*, 40:452–475, 2013.

- [19] Gene H Golub, Michael Heath, and Grace Wahba. Generalized cross-validation as a method for choosing a good ridge parameter. *Technometrics*, 21(2):215–223, 1979.
- [20] Gene H. Golub and Charles F. van Loan. *Matrix computations*. Johns Hopkins Press, Baltimore, 3rd edition, 1996.
- [21] G.H. Golub and C.F. Van Loan. *Matrix Computations*. Johns Hopkins Studies in the Mathematical Sciences. Johns Hopkins University Press, 2013.
- [22] E Haber and L Tenorio. Learning regularization functionals-a supervised training approach. *Inverse Problems*, 19:611–626, June 2003.
- [23] Per Christian Hansen. Analysis of discrete ill-posed problems by means of the L-curve. *SIAM Review*, 34:561–580, 1992.
- [24] Per Christian Hansen. *Rank-Deficient and Discrete Ill-Posed Problems*. Society for Industrial and Applied Mathematics, Philadelphia, 1998.
- [25] Per Christian Hansen, James G Nagy, and Dianne P O’Leary. *Deblurring Images: Matrices, Spectra, and Filtering*. Fundamentals of Algorithms. Society for Industrial and Applied Mathematics, Philadelphia, 2006.
- [26] Per Christian Hansen and Dianna P. O’Leary. The use of the L-curve in the regularization of discrete ill-posed problems. *SIAM J. Sci. Comput.*, 14:1487–1503, 1993.
- [27] Gernot Holler and Karl Kunisch. Learning nonlocal regularization operators, January 2020. Optimization and Control: arXiv:2001.09092.
- [28] Gareth James, Daniela Witten, Trevor Hastie, and Robert Tibshirani. *An Introduction to Statistical Learning with Applications in R*. Springer, 2013.
- [29] Martti Kalke and Samuli Siltanen. Adaptive frequency-domain regularization for sparse-data tomography. *Inverse Problems in Science and Engineering*, 21:1099–1124, 10 2013.
- [30] Karl Kunisch and Thomas Pock. A bilevel optimization approach for parameter learning in variational models. *SIAM Journal on Imaging Sciences*, 6(2):938–983, 2013.
- [31] Randall J LeVeque. *Finite Difference Methods for Ordinary and Partial Differential Equations: Steady-State and Time-Dependent Problems*. SIAM, 2007.
- [32] S Lu and S V Pereverzev. Multi-parameter regularization and its numerical realization. *Numerische Mathematik*, 118:1–31, 2011.
- [33] Colin Lingwood Mallows. Some comments on c_p . *Technometrics*, 15(4):661–675, November 1973.
- [34] Jodi L Mead. Parameter estimation: A new approach to weighting a priori information. *Journal of Inverse and Ill-posed Problems*, 16:175–193, 2008.
- [35] Jodi L Mead and Rosemary A Renaut. A Newton root-finding algorithm for estimating the regularization parameter for solving ill-conditioned least squares problems. *Inverse Problems*, 25(2):025002, 2009.

- [36] Kourosh Modarresi and Gene Golub. Multi-level approach to numerical solution of inverse problems. In *CSC 2007: SIAM Workshop on Combinatorial Scientific Computing*. IEEE Computer Society, 2007.
- [37] Kourosh Modarresi and Gene Golub. Using multiple generalized cross-validation as a method for varying smoothing effects. In *CSC 2007: SIAM Workshop on Combinatorial Scientific Computing*. SIAM, IEEE Computer Society, 2007.
- [38] Vladimir Alekseevich Morozov. On the solution of functional equations by the method of regularization. *Soviet Mathematics Doklady*, 7:414–417, 1966.
- [39] NASA and JPL-Caltech. Photojournal: Mercury, 2016.
- [40] Michael K. Ng, Raymond H. Chan, and Wun-Cheung Tang. A fast algorithm for deblurring models with Neumann boundary conditions. *SIAM Journal on Scientific Computing*, 21(3):851–866, 1999.
- [41] Christopher C. Paige and Michael A. Saunders. Towards a generalized singular value decomposition. *SIAM Journal on Numerical Analysis*, 18(3):398–405, 1981.
- [42] R. A. Renaut. A parallel multisplitting solution of the least squares problem. *Numerical Linear Algebra with Applications*, pages 11–31, 1998.
- [43] R. A. Renaut, S. Vatankehah, and V. E. Ardestani. Hybrid and iteratively reweighted regularization by unbiased predictive risk and weighted GCV for projected systems. *SIAM J. Sci. Comput.*, 39:B221–B243., 2017.
- [44] Rosemary A. Renaut, Youzuo Lin, and Hongbin Guo. Multisplitting for regularized least squares with Krylov subspace recycling. *Numerical Linear Algebra with Applications*, 19(4):655–676, 2012.
- [45] Jenni A M Sidey-Gibbons and Chris J. Sidey-Gibbons. Machine learning in medicine: a practical introduction. *BMC Medical Research Methodology*, 19, 2019.
- [46] I. M. Stephanakis and S. Kollias. Generalized-cross-validation estimation of the regularization parameters of the subbands in wavelet domain regularized image restoration. In *Conference Record of Thirty-Second Asilomar Conference on Signals, Systems and Computers (Cat. No.98CH36284)*, volume 2, pages 938–940 vol.2, 1998.
- [47] Gilbert Strang. The discrete cosine transform. *SIAM Review*, 41(1):135–147, January 1999.
- [48] Viktoria Taroudaki and Dianne P. O’Leary. Near-optimal spectral filtering and error estimation for solving ill-posed problems. *SIAM Journal on Scientific Computing*, 37(6):A2947–A2968, 2015.
- [49] A. N. Tikhonov. Regularization of incorrectly posed problems. *Soviet Mathematics Doklady*, 4:1624–1627, 1963.

- [50] Saeed Vatanikhah, Rosemary A. Renaut, and Vahid E. Ardestani. A fast algorithm for regularized focused 3-D inversion of gravity data using the randomized SVD. *Geophysics*, 83::G25–G34, 2018.
- [51] Saeed Vatanikhah, Rosemary A Renaut, and Vahid E Ardestani. Total variation regularization of the 3-d gravity inverse problem using a randomized generalized singular value decomposition. *Geophysical Journal International*, 213(1):695–705, 2018.
- [52] E De Vito, L Rosasco, A Caponnetto, U Giovannini, and F Odone. Learning from examples as an inverse problem. *Journal of Machine Learning Research*, 6:883–904, 2005.
- [53] Curt Vogel. *Computational Methods for Inverse Problems*. Society for Industrial and Applied Mathematics, Philadelphia, 2002.
- [54] Grace Wahba. Practical approximate solutions to linear operator equations when the data are noisy. *SIAM Journal on Numerical Analysis*, 14(4):651–667, September 1977.
- [55] Grace Wahba. *Spline Models for Observational Data*, chapter Estimating the Smoothing Parameter, pages 52–62. CBMS-NSF Regional Conference Series in Applied Mathematics. SIAM, 1990.
- [56] Z Wang. Multi-parameter Tikhonov regularization and model function approach to the damped Morozov principle for choosing regularization parameters. *Journal of Computational and Applied Mathematics*, 236:1815–1832, 2012.
- [57] S N Wood. Modelling and smoothing parameter estimation with multiple quadratic penalties. *Journal of the Royal Statistical Society: Series B*, 62:413–428, January 2002.
- [58] J. M. Zobitz, Tristan Quaife, and Nancy K. Nichols. Efficient hyper-parameter determination for regularised linear BRDF parameter retrieval. *International Journal of Remote Sensing*, 41:1437 – 1457, 2020.

A The Unbiased Predictive Risk Estimator for Windowed Tikhonov

We briefly describe the derivation of the UPRE in the context of learning regularization parameters from multiple data sets and using spectral windowing. This mimics the derivation in [53, p. 98] but in all cases assumes that the matrices and vectors are for multiple data sets and that regularization parameters are defined with respect to spectral windows. For ease of notation we drop the $\tilde{\mathbf{A}}$ notation, and we drop the dependence on $\boldsymbol{\alpha}$ in all terms. Also we assume that the noise in the measured data is independent so that the covariance matrix for the noise, $\boldsymbol{\Sigma}$, is diagonal, where $\boldsymbol{\eta} \sim \mathcal{N}(0, \boldsymbol{\Sigma})$. We now proceed to obtain the proof of Theorem 3.1 from first principles.

Proof. Using $\mathbf{x}(\alpha) = \mathbf{A}_{\text{win}}^\# \mathbf{d}$ we have

$$\begin{aligned}\mathbf{r}(\alpha) &= (\mathbf{A}\mathbf{A}_{\text{win}}^\# - \mathbf{I}_M)\mathbf{d} = (\mathbf{A}\mathbf{A}_{\text{win}}^\# - \mathbf{I}_M)\mathbf{b} + (\mathbf{A}\mathbf{A}_{\text{win}}^\# - \mathbf{I}_M)\boldsymbol{\eta} \text{ and} \\ \mathbf{p}(\alpha) &= (\mathbf{A}\mathbf{A}_{\text{win}}^\# - \mathbf{I}_M)\mathbf{b} + \mathbf{A}\mathbf{A}_{\text{win}}^\# \boldsymbol{\eta}.\end{aligned}$$

Here \mathbf{I}_M is defined consistently for the size of the problem, $M = \sum_{r=1}^R m_r$. In both cases we have a linear combination between $\mathbf{f} = (\mathbf{A}\mathbf{A}_{\text{win}}^\# - \mathbf{I}_M)\mathbf{b}$ which is deterministic and a noise term $\mathbf{B}\boldsymbol{\eta}$, where $\mathbf{B} = \mathbf{A}\mathbf{A}_{\text{win}}^\#$ or $\mathbf{B} = (\mathbf{A}\mathbf{A}_{\text{win}}^\# - \mathbf{I}_M)$. Now by the Trace Lemma [53, Lemma 7.2] we have

$$E(\|\mathbf{f} + \mathbf{B}\boldsymbol{\eta}\|_2^2) = E(\|\mathbf{f}\|_2^2) + \text{trace}(\mathbf{B}^\top \mathbf{B} \boldsymbol{\Sigma}). \quad (42)$$

Here $E(a)$ denotes the expectation of a . Thus, applying eq. (42) twice we have

$$\begin{aligned}E(\|\mathbf{r}(\alpha)\|_2^2) &= E(\|\mathbf{f}\|_2^2) + \text{trace}((\mathbf{A}\mathbf{A}_{\text{win}}^\#)^\top \mathbf{A}\mathbf{A}_{\text{win}}^\# \boldsymbol{\Sigma}) \\ &\quad + \text{trace}(\boldsymbol{\Sigma}) - \text{trace}(\mathbf{A}\mathbf{A}_{\text{win}}^\# \boldsymbol{\Sigma}) - \text{trace}((\mathbf{A}\mathbf{A}_{\text{win}}^\#)^\top \boldsymbol{\Sigma}) \text{ and} \\ E(\|\mathbf{p}(\alpha)\|_2^2) &= E(\|\mathbf{f}\|_2^2) + \text{trace}((\mathbf{A}\mathbf{A}_{\text{win}}^\#)^\top \mathbf{A}\mathbf{A}_{\text{win}}^\# \boldsymbol{\Sigma}).\end{aligned}$$

Immediately, approximating $E(\|\mathbf{r}(\alpha)\|_2^2)$ by $\|\mathbf{r}(\alpha)\|_2^2$ as in the single parameter derivation, and assuming that $\mathbf{A}\mathbf{A}_{\text{win}}^\#$ is symmetric, yields the estimator

$$E\left(\frac{1}{M}\|\mathbf{p}(\alpha)\|_2^2\right) \approx \frac{1}{M} \left(\|\mathbf{r}(\alpha)\|_2^2 - \text{trace}(\boldsymbol{\Sigma}) + 2 \text{trace}(\mathbf{A}\mathbf{A}_{\text{win}}^\# \boldsymbol{\Sigma}) \right). \quad (43)$$

For multiple data sets the system matrices are block diagonal and the systems decouple. Hence $\|\mathbf{r}(\alpha)\|_2^2 = \sum_{r=1}^R \|\mathbf{r}^{(r)}(\alpha)\|_2^2$ and

$$\text{trace}(\mathbf{A}\mathbf{A}_{\text{win}}^\# \boldsymbol{\Sigma}) = \sum_{r=1}^R \text{trace}(\mathbf{A}^{(r)}(\mathbf{A}_{\text{win}}^{(r)})^\# \boldsymbol{\Sigma}_r).$$

Therefore,

$$\begin{aligned}E\left(\frac{1}{M}\|\mathbf{p}(\alpha)\|_2^2\right) &\approx \frac{1}{M} \sum_{r=1}^R \left(\|\mathbf{r}^{(r)}(\alpha)\|_2^2 - \text{trace}(\boldsymbol{\Sigma}_r) + 2 \text{trace}(\mathbf{A}^{(r)}(\mathbf{A}_{\text{win}}^{(r)})^\# \boldsymbol{\Sigma}_r) \right) \\ &= \frac{1}{M} \sum_{r=1}^R m_r F_{\text{UPRE}}^{(r)}(\alpha),\end{aligned}$$

where the last equality results by applying eq. (43) for each system r . As a consequence we have the proof of the estimator given in Theorem 3.1 under the assumption that $\mathbf{A}\mathbf{A}_{\text{win}}^\#$ is symmetric

$$E\left(\frac{1}{M}\|\mathbf{p}(\alpha)\|_2^2\right) \approx \frac{1}{M} \sum_{r=1}^R \left(\|\mathbf{r}^{(r)}(\alpha)\|_2^2 - \text{trace}(\boldsymbol{\Sigma}_r) + 2 \text{trace}(\mathbf{A}^{(r)}(\mathbf{A}_{\text{win}}^{(r)})^\# \boldsymbol{\Sigma}_r) \right).$$

□

When we have the GSVD for each system it is immediate, with or without windowing, that

$$\mathbf{A}\mathbf{A}_{\text{win}}^\# = \mathbf{U} \sum_{p=1}^P \left(W^{(p)} \right)^{1/2} \Delta (\Delta^\top \Delta + \alpha_p^2 \Lambda^\top \Lambda)^{-1} \Delta^\top (W^{(p)})^{1/2} \mathbf{U}^\top, \quad (44)$$

is symmetric for each block and/or window.

B Generalized Cross Validation for Windowed Tikhonov

We now consider the direct derivation from first principles for the generalized Tikhonov regularized problem. Following the approach in [11], and using eq. (5), we consider the solution using the spectral domain coefficients

$$\mathbf{y} = \mathbf{X}^\top \mathbf{x}(\alpha) = \mathbf{\Phi}(\alpha) \mathbf{\Delta}^\dagger \hat{\mathbf{d}}, \quad (45)$$

which corresponds to the solution of the normal equations

$$(\mathbf{\Delta}^\top \mathbf{\Delta} + \alpha^2 \mathbf{\Lambda}^\top \mathbf{\Lambda}) \mathbf{y} = \mathbf{\Delta}^\top \hat{\mathbf{d}}, \quad (46)$$

for the regularized problem

$$\|\mathbf{\Delta} \mathbf{y} - \hat{\mathbf{d}}\|_2^2 + \alpha^2 \|\mathbf{\Lambda} \mathbf{y}\|_2^2. \quad (47)$$

As in [11, 19], we introduce \mathbf{C} as the unitary matrix which diagonalizes the circulants and consider the new system $\mathbf{G} \mathbf{y} \approx \mathbf{C} \hat{\mathbf{d}}$, where $\mathbf{G} = \mathbf{C} \mathbf{\Delta}$ is of size $m \times n$. For this new system \mathbf{y} solves

$$(\mathbf{G}^\top \mathbf{G} + \alpha^2 \mathbf{\Lambda}^\top \mathbf{\Lambda}) \mathbf{y} = \mathbf{G}^\top \mathbf{C} \hat{\mathbf{d}},$$

and the corresponding windowed solution is given by

$$\mathbf{y}_{\text{win}} = \sum_{p=1}^P (\mathbf{G}^\top \mathbf{G} + \alpha_p^2 \mathbf{\Lambda}^\top \mathbf{\Lambda})^{-1} \mathbf{W}^{(p)} \mathbf{G}^\top \mathbf{C} \hat{\mathbf{d}}. \quad (48)$$

Following [11] but consistent with our notation introduced in eq. (3) applied for the solution in the spectral domain we introduce the data resolution matrices

$$\begin{aligned} \mathbf{G}(\alpha_p) &= \mathbf{G}(\mathbf{G}^\top \mathbf{G} + \alpha_p^2 \mathbf{\Lambda}^\top \mathbf{\Lambda})^{-1} \mathbf{G}^\top = \mathbf{G} \mathbf{G}^\#(\alpha_p) \text{ and} \\ \mathbf{G}_{\text{win}(p)}(\alpha_p) &= \mathbf{G}(\mathbf{G}^\top \mathbf{G} + \alpha_p^2 \mathbf{\Lambda}^\top \mathbf{\Lambda})^{-1} \mathbf{W}^{(p)} \mathbf{G}^\top = \mathbf{G} \mathbf{G}_{\text{win}(p)}^\#(\alpha_p). \end{aligned}$$

In the derivation we will need the diagonal entries related to these resolution matrices.

Lemma B.1 (Diagonal entries of resolution matrices). *The diagonal entries of the matrices $\mathbf{I}_m - \mathbf{G} \mathbf{G}^\#(\alpha_p)$ and $\mathbf{I}_m - \mathbf{G} \mathbf{G}_{\text{win}(p)}^\#(\alpha_p)$ denoted by $\mu^{(p)}$ and $\nu^{(p)}$ are given by*

$$\begin{aligned} \mu^{(p)} &= \frac{1}{m} \left(m - n + \sum_{j=1}^n (1 - \Phi_{jj}(\alpha_p)) \right) \text{ and} \\ \nu^{(p)} &= \frac{1}{m} \left(m - n + \sum_{j=1}^n (1 - (\Phi_{\text{win}(p)})_{jj}(\alpha_p)) \right). \end{aligned}$$

Proof. We substitute back in for \mathbf{G} and note that the filter matrices are of sizes $n \times n$

$$\mathbf{G} \mathbf{G}^\#(\alpha_p) = \mathbf{C} \mathbf{\Delta} (\mathbf{\Delta}^\top \mathbf{\Delta} + \alpha_p^2 \mathbf{\Lambda}^\top \mathbf{\Lambda})^{-1} \mathbf{\Delta}^\top \mathbf{C}^* = \mathbf{C} \begin{bmatrix} \Phi(\alpha_p) & 0 \\ 0 & 0 \end{bmatrix} \mathbf{C}^*.$$

Also

$$\mathbf{I}_m - \mathbf{G}\mathbf{G}^\#(\alpha_p) = \mathbf{C} \left(\mathbf{I}_m - \begin{bmatrix} \Phi(\alpha_p) & 0 \\ 0 & 0 \end{bmatrix} \right) \mathbf{C}^* = \mathbf{C} \begin{bmatrix} \mathbf{I}_n - \Phi(\alpha_p) & 0 \\ 0 & \mathbf{I}_{m-n} \end{bmatrix} \mathbf{C}^*,$$

is circulant since the inner part of this product is diagonal. Therefore, its diagonal entries are equal and we can write $\text{diag}(\mathbf{I}_m - \mathbf{G}\mathbf{G}^\#(\alpha_p)) = \mu^{(p)} \mathbf{I}_m$. Further, since \mathbf{C} is unitary

$$\text{trace}(\mathbf{I}_m - \mathbf{G}\mathbf{G}^\#(\alpha_p)) = \sum_{j=1}^n (1 - \Phi_{jj}(\alpha_p)) + (m - n), \quad (49)$$

and

$$\mu^{(p)} = \frac{1}{m} \left(m - n + \sum_{j=1}^n (1 - \Phi_{jj}(\alpha_p)) \right).$$

The result for the diagonal entries of $\mathbf{G}_{\text{win}(p)}(\alpha_p)$ follows similarly. \square

Equipped with this result, we now proceed with the proof of Theorem 3.2.

Proof. To obtain $F_{\text{GCV}}(\boldsymbol{\alpha})$ relies on deriving the Allen PRESS estimates [19]

$$F(\boldsymbol{\alpha}) = \frac{1}{m} \sum_{k=1}^m \left((\mathbf{C}\hat{\mathbf{d}})_k - (\mathbf{G}\mathbf{y}_{\text{win}}^{(k)})_k \right)^2,$$

where $\mathbf{y}_{\text{win}}^{(k)}$ is the solution of eq. (48) with the k^{th} equation removed and $(\mathbf{a})_k$ indicates the k^{th} component of a vector \mathbf{a} . To find $\mathbf{y}_{\text{win}}^{(k)}$, we remove row k from matrix \mathbf{G} when forming eq. (48). As in [11] this is accomplished using multiplication by matrix $\mathbf{E}_k = \mathbf{I}_m - \mathbf{e}_k \mathbf{e}_k^\top$. But now, from the form of \mathbf{G} we obtain $\mathbf{E}_k \mathbf{G} = \mathbf{E}_k \mathbf{C} \boldsymbol{\Delta} = (\mathbf{I}_m - \mathbf{e}_k \mathbf{e}_k^\top) \mathbf{C} \boldsymbol{\Delta}$. But $\mathbf{e}_k^\top \mathbf{C} = \mathbf{c}_k^\top$ is the k^{th} row of \mathbf{C} . Because \mathbf{C} is unitary this gives $\mathbf{G}^\top \mathbf{E}_k^\top \mathbf{E}_k \mathbf{G} = \boldsymbol{\Delta}^\top \boldsymbol{\Delta} - \boldsymbol{\Delta}^\top \mathbf{c}_k \mathbf{c}_k^\top \boldsymbol{\Delta}$. Therefore,

$$\mathbf{G}^\top \mathbf{E}_k^\top \mathbf{E}_k \mathbf{G} + \alpha_p^2 \boldsymbol{\Lambda}^\top \boldsymbol{\Lambda} = \boldsymbol{\Delta}^\top \boldsymbol{\Delta} + \alpha_p^2 \boldsymbol{\Lambda}^\top \boldsymbol{\Lambda} - \boldsymbol{\Delta}^\top \mathbf{c}_k \mathbf{c}_k^\top \boldsymbol{\Delta} = \mathbf{H}(\alpha_p) - \mathbf{h}_k \mathbf{h}_k^\top,$$

which defines diagonal matrix $\mathbf{H}(\alpha_p)$ and $\mathbf{h}_k = \boldsymbol{\Delta}^\top \mathbf{c}_k = \boldsymbol{\Delta}^\top \mathbf{C}^* \mathbf{e}_k$. This is a rank one update for the matrix $\mathbf{H}(\alpha_p)$ and the Sherman-Morrison formula [21, Equation 2.1.5] gives

$$(\mathbf{H}(\alpha_p) - \mathbf{h}_k \mathbf{h}_k^\top)^{-1} = \mathbf{H}(\alpha_p)^{-1} + \frac{1}{\beta_k} \mathbf{H}(\alpha_p)^{-1} \mathbf{h}_k \mathbf{h}_k^\top \mathbf{H}(\alpha_p)^{-1},$$

where $\beta_k = 1 - \mathbf{h}_k^\top \mathbf{H}(\alpha_p)^{-1} \mathbf{h}_k = \mu^{(p)}$ is independent of k as already shown in Lemma B.1. Now $(\mathbf{G}\mathbf{y}_{\text{win}}^{(k)})_k$ is a sum over the p windows of terms that involve

$$\begin{aligned} \mathbf{e}_k^\top \mathbf{C} \boldsymbol{\Delta} (\mathbf{H}(\alpha_p) - \mathbf{h}_k \mathbf{h}_k^\top)^{-1} &= \mathbf{h}_k^\top \left(\mathbf{H}(\alpha_p)^{-1} + \frac{1}{\mu^{(p)}} \mathbf{H}(\alpha_p)^{-1} \mathbf{h}_k \mathbf{h}_k^\top \mathbf{H}(\alpha_p)^{-1} \right) \\ &= \left(1 + \frac{1}{\mu^{(p)}} \mathbf{h}_k^\top \mathbf{H}(\alpha_p)^{-1} \mathbf{h}_k \right) \mathbf{h}_k^\top \mathbf{H}(\alpha_p)^{-1} = \frac{\mathbf{h}_k^\top \mathbf{H}(\alpha_p)^{-1}}{\mu^{(p)}} \\ &= \frac{\mathbf{h}_k^\top}{\mu^{(p)}} (\boldsymbol{\Delta}^\top \boldsymbol{\Delta} + \alpha_p^2 \boldsymbol{\Lambda}^\top \boldsymbol{\Lambda})^{-1}. \end{aligned}$$

Therefore,

$$\begin{aligned} (\mathbf{G}\mathbf{y}_{\text{win}}^{(k)})_k &= \mathbf{e}_k^\top \sum_{p=1}^P \frac{1}{\mu^{(p)}} \mathbf{C} \mathbf{\Delta} (\mathbf{\Delta}^\top \mathbf{\Delta} + \alpha_p^2 \mathbf{\Lambda}^\top \mathbf{\Lambda})^{-1} \mathbf{W}^{(p)} \mathbf{\Delta}^\top \mathbf{C}^* \mathbf{E}_k \mathbf{C} \hat{\mathbf{d}}, \\ &= \mathbf{e}_k^\top \mathbf{C} \left(\sum_{p=1}^P \frac{1}{\mu^{(p)}} \begin{bmatrix} \Phi_{\text{win}^{(p)}}(\alpha_p) & 0 \\ 0 & 0 \end{bmatrix} - \frac{1 - \nu^{(p)}}{\mu^{(p)}} \mathbf{I}_m \right) \hat{\mathbf{d}}, \end{aligned}$$

and

$$(\mathbf{C}\hat{\mathbf{d}})_k - (\mathbf{G}\mathbf{y}_{\text{win}}^{(k)})_k = \mathbf{e}_k^\top \mathbf{C} \left(\mathbf{I}_m - \left(\sum_{p=1}^P \frac{1}{\mu^{(p)}} \begin{bmatrix} \Phi_{\text{win}^{(p)}}(\alpha_p) & 0 \\ 0 & 0 \end{bmatrix} + \frac{1 - \nu^{(p)}}{\mu^{(p)}} \mathbf{I}_m \right) \right) \hat{\mathbf{d}}.$$

Finally,

$$\begin{aligned} F(\alpha) &= \frac{1}{m} \left\| \left(\mathbf{I}_m - \left(\sum_{p=1}^P \frac{1}{\mu^{(p)}} \begin{bmatrix} \Phi_{\text{win}^{(p)}}(\alpha_p) & 0 \\ 0 & 0 \end{bmatrix} + \frac{1 - \nu^{(p)}}{\mu^{(p)}} \mathbf{I}_m \right) \right) \hat{\mathbf{d}} \right\|^2 \\ &= \frac{1}{m} \left(\sum_{j=q^*+1}^m \left(1 + \left(\sum_{p=1}^P \frac{1 - \nu^{(p)}}{\mu^{(p)}} \right) \right)^2 \hat{d}_j^2 + \right. \\ &\quad \left. \sum_{j=1}^{q^*} \left(1 + \left(\sum_{p=1}^P \frac{1 - \nu^{(p)}}{\mu^{(p)}} \right) - \left(\sum_{p=1}^P \frac{1}{\mu^{(p)}} \frac{\gamma_j^2 w_j^{(p)}}{\gamma_j^2 + \alpha_p^2} \right) \right)^2 \hat{d}_j^2 \right). \end{aligned}$$

□

We note that this result is consistent with the derivation using the standard form when $q^* = q < n$ [8] and with the result in [11, Theorem 3.2], when applied for the standard Tikhonov regularization.

C Algebraic Results

Derivations for the terms needed to evaluate the regularization functions are provided. It is immediate that the common feature of the standard methods eqs. (19) and (33), and their extensions, is the need to evaluate $\|\mathbf{r}\|_2^2$ and $\text{trace}(\mathbf{A}(\alpha))$. We present the results for the windowed formulations, first focusing on the residual and then the trace, and in all cases assuming $m \geq n$. The results rely on the structure of the filter matrix Φ_{win} . First we introduce $\Psi = \mathbf{I}_n - \Phi$, with entries

$$\Psi_{jj} = \begin{cases} 1 & j = 1 : \ell \quad (\delta_j = 0) \\ \frac{\alpha^2 \lambda_j^2}{\delta_j^2 + \alpha^2 \lambda_j^2} & j = \ell + 1 : q^* \\ 0 & j = q^* : n \quad (\lambda_j = 0). \end{cases} \quad (50)$$

Lemma C.1 (Components of windowed data resolution matrix).

$$\mathbf{I}_m - \mathbf{A}\mathbf{A}_{\text{win}}^\dagger = \mathbf{U} \left(\begin{bmatrix} \sum_{p=1}^P \mathbf{W}^{(p)} \Psi(\alpha_p) & 0 \\ 0 & \mathbf{I}_{m-n} \end{bmatrix} \right) \mathbf{U}^\top. \quad (51)$$

Proof. Using the GSVD and eq. (44)

$$\begin{aligned}\mathbf{I}_m - \mathbf{A}\mathbf{A}_{\text{win}}^\# &= \mathbf{I}_m - \mathbf{U} \left(\sum_{p=1}^P \mathbf{W}^{(p)} \Delta (\Delta^\top \Delta + \alpha_p^2 \Lambda^\top \Lambda)^{-1} \Delta^\top \right) \mathbf{U}^\top \\ &= \mathbf{I}_m - \mathbf{U} \left(\begin{bmatrix} \sum_{p=1}^P \Phi_{\text{win}^{(p)}} & 0 \\ 0 & 0 \end{bmatrix} \right) \mathbf{U}^\top.\end{aligned}\quad (52)$$

But now examining the components we have

$$1 - \sum_{p=1}^P w_j^{(p)} \frac{\delta_j^2}{\delta_j^2 + \alpha_p^2 \lambda_j^2} = \begin{cases} 1 & j = 1 : \ell \\ \sum_{p=1}^P w_j^{(p)} \frac{\alpha_p^2 \lambda_j^2}{\delta_j^2 + \alpha_p^2 \lambda_j^2} & j = \ell + 1 : q^* \\ 0 & j = q^* : n. \end{cases} \quad (53)$$

Therefore, the weighted filter matrix in eq. (51) follows by comparing eq. (53) with eq. (50) and by noting in addition that the entries are 1 for $j = n + 1 : m$. \square

Lemma C.1 also applies for the complex spectral decomposition replacing \mathbf{U}^\top by \mathbf{U}^* for unitary \mathbf{U} and with entries δ_j^2 and λ_j^2 replaced by $|\delta_j|^2$ and $|\lambda_j|^2$, respectively. The next results follow immediately from Lemma C.1 and are given with minimal verification or without proof.

Lemma C.2 (Norm of windowed residual). *For the windowed residual given by $\mathbf{r}_{\text{win}}(\boldsymbol{\alpha}) = \mathbf{A}\mathbf{x}_{\text{win}}(\boldsymbol{\alpha}) - \mathbf{d}$,*

$$\|\mathbf{r}_{\text{win}}(\boldsymbol{\alpha})\|_2^2 = \sum_{j=1}^{q^*} \left(\sum_{p=1}^P w_j^{(p)} \Psi_{jj}(\alpha_p) \hat{d}_j \right)^2 + \sum_{j=n+1}^m \hat{d}_j^2.$$

For non-overlapping windows with $w_j^{(p)} = 1$ for $j \in \text{win}^{(p)}$

$$\|\mathbf{r}_{\text{win}}(\boldsymbol{\alpha})\|_2^2 = \sum_{p=1}^P \sum_{j \in \text{win}^{(p)}} \left(\Psi_{jj}(\alpha_p) \hat{d}_j \right)^2 + \sum_{j=n+1}^m \hat{d}_j^2 = \sum_{p=1}^P \|\hat{\mathbf{r}}_{\text{win}}^{(p)}(\alpha_p)\|_2^2 + \sum_{j=n+1}^m \hat{d}_j^2,$$

using the definition for the windowed residual based on the spectral domain given by $\hat{\mathbf{r}}_{\text{win}}^{(p)}(\alpha_p) = \mathbf{U}^\top \mathbf{A}\mathbf{x}^{(p)}(\alpha_p) - \mathbf{W}^{(p)} \mathbf{U}^\top \mathbf{d}$.

Proof. The general result is immediate. For the non-overlapping case using the definition for the spectral residual with the definition for the windowed solution we have

$$\|\hat{\mathbf{r}}_{\text{win}}^{(p)}(\alpha_p)\|_2^2 = \|\mathbf{U}^\top \mathbf{A}\mathbf{x}^{(p)}(\alpha_p) - \mathbf{W}^{(p)} \mathbf{U}^\top \mathbf{d}\|_2^2 \quad (54)$$

$$= \|(\Delta \Phi(\alpha_p) \Delta^\dagger - \mathbf{I}_m) \mathbf{W}^{(p)} \hat{\mathbf{d}}\|^2 = \sum_{j \in \text{win}^{(p)}} \left(\Psi_{jj}(\alpha_p) \hat{d}_j \right)^2, \quad (55)$$

and the result holds. \square

Lemma C.3 (Windowed Trace).

$$\text{trace}(\mathbf{A}\mathbf{A}_{\text{win}}^\#) = (n - q^*) + \sum_{j=\ell+1}^{q^*} \sum_{p=1}^P w_j^{(p)} \Phi_{jj}(\alpha_p).$$

For non-overlapping windows

$$\text{trace}(\mathbf{A}\mathbf{A}_{\text{win}}^\#) = (n - q^*) + \sum_{p=1}^P \sum_{j \in \text{win}(p)} \Phi_{jj}(\alpha_p).$$

D The GSVD and the DCT

We outline the proof of Theorem 4.1.

Proof. We begin by setting $\mathbf{C}^\top \tilde{\mathbf{\Delta}} \mathbf{C} = \mathbf{U} \mathbf{\Delta} \mathbf{Z}^\top$ and rearranging terms to obtain $\mathbf{\Delta} = \mathbf{U}^\top \mathbf{C}^\top \tilde{\mathbf{\Delta}} \mathbf{C} \mathbf{Z}^{-\top}$. Doing the same for $\tilde{\mathbf{\Lambda}}$, and using $\mathbf{\Delta}^\top \mathbf{\Delta} + \tilde{\mathbf{\Lambda}}^\top \tilde{\mathbf{\Lambda}} = \mathbf{I}_n$, we have

$$\mathbf{Z}^{-1} \mathbf{C}^\top \tilde{\mathbf{\Delta}}^\top \tilde{\mathbf{\Delta}} \mathbf{C} \mathbf{Z}^{-\top} + \mathbf{Z}^{-1} \mathbf{C}^\top \tilde{\mathbf{\Lambda}}^\top \tilde{\mathbf{\Lambda}} \mathbf{C} \mathbf{Z}^{-\top} = \mathbf{I}_n,$$

from which we have

$$\tilde{\mathbf{\Delta}}^\top \tilde{\mathbf{\Delta}} + \tilde{\mathbf{\Lambda}}^\top \tilde{\mathbf{\Lambda}} = \mathbf{C} \mathbf{Z} \mathbf{Z}^\top \mathbf{C}^\top.$$

Since $\text{null}(\mathbf{A}) \cap \text{null}(\mathbf{L}) = \{\mathbf{0}\}$, the matrix on the left is diagonal with positive entries. Thus, we can form the (positive) square root $\mathbf{S} = \sqrt{\tilde{\mathbf{\Delta}}^\top \tilde{\mathbf{\Delta}} + \tilde{\mathbf{\Lambda}}^\top \tilde{\mathbf{\Lambda}}}$ which is also diagonal with positive entries. Using \mathbf{S} we can write $\mathbf{S}^2 = \mathbf{S} \mathbf{S}^\top = \mathbf{C} \mathbf{Z} \mathbf{Z}^\top \mathbf{C}^\top$, which implies that we can set $\mathbf{Z} = \mathbf{C}^\top \mathbf{S}$; \mathbf{S} is invertible but not necessarily orthogonal, so \mathbf{Z} is only invertible. Using the transpose $\mathbf{Z}^\top = \mathbf{S} \mathbf{C}$ and inverse \mathbf{S}^{-1} , we can then write

$$\mathbf{A} = \mathbf{C}^\top \tilde{\mathbf{\Delta}} \mathbf{S}^{-1} \mathbf{S} \mathbf{C} = \mathbf{C}^\top \tilde{\mathbf{\Delta}} \mathbf{S}^{-1} \mathbf{Z}^\top \text{ and } \mathbf{L} = \mathbf{C}^\top \tilde{\mathbf{\Lambda}} \mathbf{S}^{-1} \mathbf{S} \mathbf{C} = \mathbf{C}^\top \tilde{\mathbf{\Lambda}} \mathbf{S}^{-1} \mathbf{Z}^\top.$$

The last step is to reorder the elements of $\tilde{\mathbf{\Delta}} \mathbf{S}^{-1}$ and $\tilde{\mathbf{\Lambda}} \mathbf{S}^{-1}$; fortunately they have the opposite order regardless of the order of the elements of $\tilde{\mathbf{\Delta}}$ and $\tilde{\mathbf{\Lambda}}$. Therefore we can use a permutation matrix \mathbf{P} so that $\mathbf{\Delta} = \mathbf{P}^\top \tilde{\mathbf{\Delta}} \mathbf{S}^{-1} \mathbf{P}$ and $\mathbf{\Lambda} = \mathbf{P}^\top \tilde{\mathbf{\Lambda}} \mathbf{S}^{-1} \mathbf{P}$ have the desired ordering. Since permutation matrices are orthogonal, we finally obtain the GSVD:

$$\begin{aligned} \mathbf{A} &= \mathbf{C}^\top \tilde{\mathbf{\Delta}} \mathbf{S}^{-1} \mathbf{Z}^\top = \mathbf{C}^\top \mathbf{P} \mathbf{P}^\top \tilde{\mathbf{\Delta}} \mathbf{S}^{-1} \mathbf{P} \mathbf{P}^\top \mathbf{Z}^\top = \mathbf{U} \mathbf{\Delta} \mathbf{X}^\top, \\ \mathbf{L} &= \mathbf{C}^\top \tilde{\mathbf{\Lambda}} \mathbf{S}^{-1} \mathbf{Z}^\top = \mathbf{C}^\top \mathbf{P} \mathbf{P}^\top \tilde{\mathbf{\Lambda}} \mathbf{S}^{-1} \mathbf{P} \mathbf{P}^\top \mathbf{Z}^\top = \mathbf{U} \mathbf{\Lambda} \mathbf{X}^\top, \end{aligned}$$

where $\mathbf{U} = \mathbf{C}^\top \mathbf{P}$ is orthogonal and $\mathbf{X} = \mathbf{Z} \mathbf{P}$ is invertible. Now it follows that $\mathbf{\Delta}^\top \mathbf{\Delta} + \mathbf{\Lambda}^\top \mathbf{\Lambda} = \mathbf{I}_n$ because

$$\begin{aligned} \mathbf{\Delta}^\top \mathbf{\Delta} + \mathbf{\Lambda}^\top \mathbf{\Lambda} &= \mathbf{P}^\top \mathbf{S}^{-\top} \tilde{\mathbf{\Delta}}^\top \tilde{\mathbf{\Delta}} \mathbf{S}^{-1} \mathbf{P} + \mathbf{P}^\top \mathbf{S}^{-\top} \tilde{\mathbf{\Lambda}}^\top \tilde{\mathbf{\Lambda}} \mathbf{S}^{-1} \mathbf{P} \\ &= \mathbf{P}^\top \mathbf{S}^{-\top} \left(\tilde{\mathbf{\Delta}}^\top \tilde{\mathbf{\Delta}} + \tilde{\mathbf{\Lambda}}^\top \tilde{\mathbf{\Lambda}} \right) \mathbf{S}^{-1} \mathbf{P} \\ &= \mathbf{P}^\top (\mathbf{S}^2)^{-1} \left(\tilde{\mathbf{\Delta}}^\top \tilde{\mathbf{\Delta}} + \tilde{\mathbf{\Lambda}}^\top \tilde{\mathbf{\Lambda}} \right) \mathbf{P} \\ &= \mathbf{P}^\top \left(\tilde{\mathbf{\Delta}}^\top \tilde{\mathbf{\Delta}} + \tilde{\mathbf{\Lambda}}^\top \tilde{\mathbf{\Lambda}} \right)^{-1} \left(\tilde{\mathbf{\Delta}}^\top \tilde{\mathbf{\Delta}} + \tilde{\mathbf{\Lambda}}^\top \tilde{\mathbf{\Lambda}} \right) \mathbf{P} = \mathbf{I}_n. \end{aligned}$$

□

The condition $\text{null}(\mathbf{A}) \cap \text{null}(\mathbf{L}) = \{\mathbf{0}\}$ in Theorem 4.1 is necessary for the property $\mathbf{\Delta}^\top \mathbf{\Delta} + \mathbf{\Lambda}^\top \mathbf{\Lambda} = \mathbf{I}_n$. While this identity is not used explicitly in any of the derivations used for finding the **UPRE** and **GCV** functions, it is standard that the mutual GSVD decomposition is obtained with this condition imposed when it is calculated using the CS decomposition, and it is therefore relevant to show that the condition still holds for the given **DCT** case [20, 3]. As an alternative, we could require that $\mathbf{\Delta}^\top \mathbf{\Delta} + \mathbf{\Lambda}^\top \mathbf{\Lambda} = \tilde{\mathbf{I}}_n$ where $\tilde{\mathbf{I}}_n$ is a modified identity matrix that has some zero diagonal elements. This generalization, as well as a conversion involving Kronecker products, is described in [8, Chapter 2]. Furthermore, equipped with Theorem 4.1, it is clear that the simplifications for the parameter selection methods using the GSVD can be rewritten in terms of the **DCT** simultaneous decomposition, which is particularly relevant for the efficient solution of two-dimensional problems. A similar approach can be used to convert the Kronecker product **DCT** for 2D problems to a GSVD.